

Materials science and architecture

Martin Bechthold¹ and James C. Weaver²

Abstract | Materiality — the use of various materials in architecture — has been fundamental to the design and construction of buildings, and materials science has traditionally responded to needs formulated by design, engineering and construction professionals. Material properties and processes are shaping buildings and influencing how they perform. The advent of technologies such as digital fabrication, robotics and 3D printing have not only accelerated the development of new construction solutions, but have also led to a renewed interest in materials as a catalyst for novel architectural design. In parallel, materials science has transformed from a field that explains materials to one that designs materials from the bottom up. The conflation of these two trends is giving rise to materials-based design research in which architects, engineers and materials scientists work as partners in the conception of new materials systems and their applications. This Review surveys this development for different material classes (wood, ceramics, metals, concrete, glass, synthetic composites and polymers), with an emphasis on recent trends and innovations.

The role of materials science in construction has traditionally been to provide new materials solutions to address problems identified by building physicists, structural engineers, architectural designers and other building specialists. This traditionally passive role is changing, in part, as materials scientists acquire the ability to design materials in a bottom-up manner to match almost any performance requirement. At the same time, designers are taking renewed interest in the exciting opportunities that advances in materials science can bring to the design table^{1,2}.

After the historical split between construction and design in the Renaissance age, engineering and architectural design evolved as separate disciplines in the 19th century³. Advances in materials development were slow, but eventually construction transitioned from the assembly of pre-shaped natural materials — wood and stone — to the systematic deployment of man-made materials, which started with ceramics, then included metals, then concrete and glass, and, more recently, engineered wood products, plastics and composites⁴. These efforts relied heavily on materials science to solve problems that emerged during the design, engineering and construction processes.

At present, the role of materials science in design is undergoing a dramatic transformation. The introduction of digital design and manufacturing technologies in the early 2000s⁵ led design professionals to consider materials design not just as a necessary means to solving construction problems; the potential of materials experimentation as a catalyst for novel design expressions was rediscovered, leading to several publications geared

towards disseminating knowledge on smart materials¹ and nanomaterials⁶ among a design and engineering audience. Experiments in materiality often involve innovative approaches to design computation and digital fabrication, and now increasingly rely on interdisciplinary teams of designers and scientists^{7,8}.

This Review traces the legacy of the major materials used in construction — wood, ceramics, metals, concrete, glass, plastics and synthetic composites — with an emphasis on recent innovations that balance technical and scientific rigor with designers' imagination. Where available, research efforts to lower the environmental impact of these materials are discussed. Not surprisingly, relative to the overall number of materials available for use, architecture uses an extremely limited palette of materials that have been industrially processed and are codified by norms and standards. By approaching design from a more fundamental, scientific perspective, design teams can create new functional and expressive applications, and, on occasion, a more sustainable use of materials. Database mappings of material properties have been created in part for the purpose of aiding scientists, engineers and designers in making more thoughtful use of materials (FIG. 1). The recent integration of sustainability metrics, such as embodied carbon and energy (the total amount of carbon or energy used in the production, distribution and use of a material), now places materials selection into a more holistic context. For example, among all building-related materials, concrete is by far the most commonly used, thus despite its relatively small carbon footprint as a function of mass, is responsible for the majority of embodied energy from construction activity.

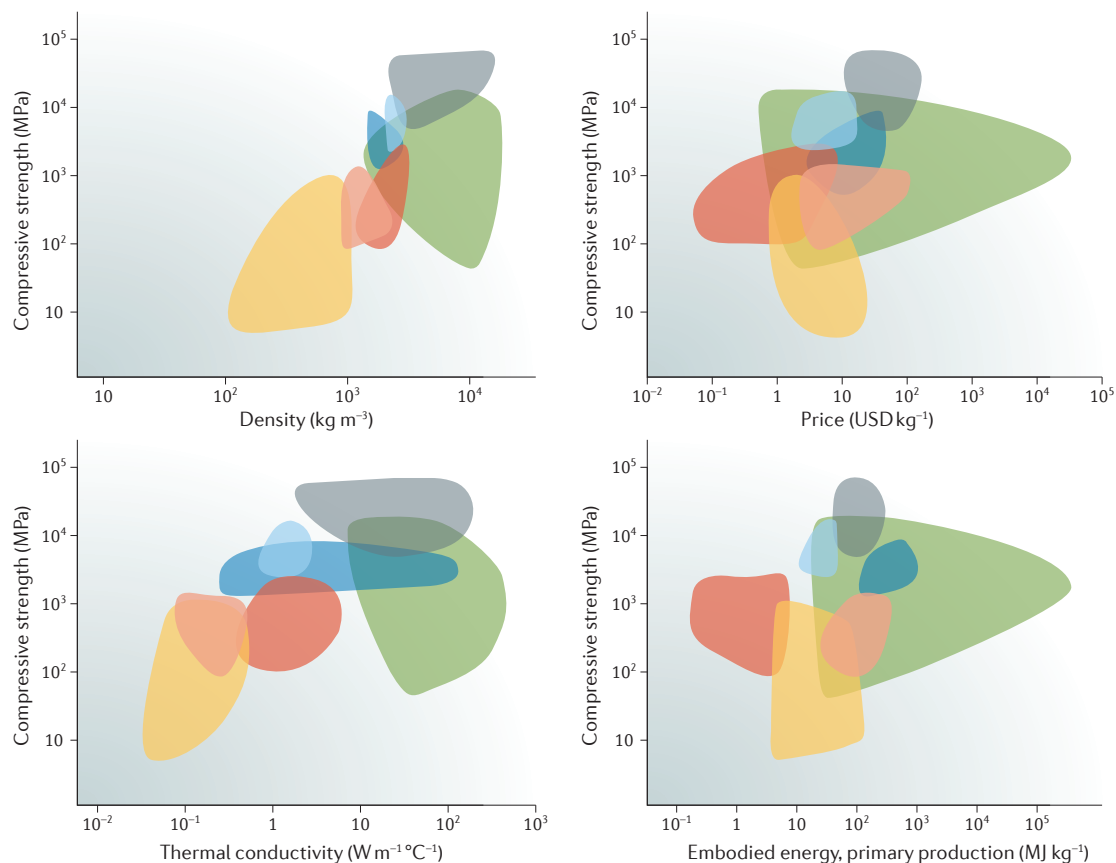
¹Graduate School of Design, Harvard University.

²Wyss Institute for Biologically Inspired Engineering, Harvard University, Cambridge, Massachusetts 02138, USA.

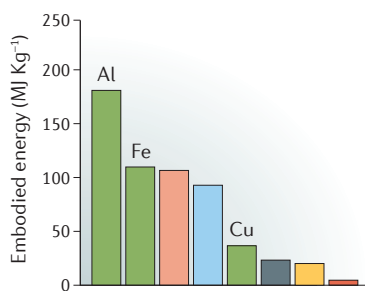
James.Weaver@wyss.harvard.edu;
mbechthold@gsd.harvard.edu

doi:10.1038/natrevmats.2017.82
Published online 5 Dec 2017

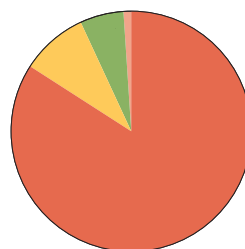
Ashby plots



Production of bulk construction materials



% Material use in construction



Average residential housing unit

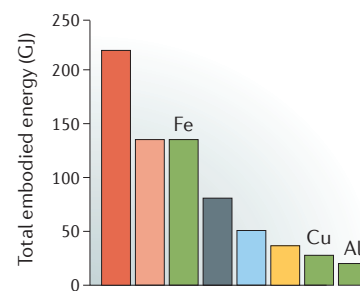


Figure 1 | Material property (Ashby) plots for different classes of construction materials. The four Ashby plots illustrate four important selection criteria for materials used in the building industry (density, price, thermal conductivity and embodied energy), plotted against compressive strength¹²⁹. Although from a materials production perspective concrete is one of the architectural materials with the lowest embodied energy, its high-percentage use results in it representing the highest total energy investment in building construction. The Ashby plots were generated using Granta CES Selector software. The pie chart is adapted with permission from REF. 114, Elsevier.

Wood

Wood (FIG. 2), a natural resource and a material that can be easily shaped with relatively simple tools, has been used in construction from the dawn of human existence. Advances in its deployment have largely been the result of better processing and shaping technologies, which were eventually complemented by the development of animal glues, first used in ancient Egypt⁹, and, in more recent times, modern synthetic adhesives. Techniques such as

sawing replaced early hand carving tools for form generation, improving shape control while reducing production waste. In the 1870s, metallurgy provided better steel for thinner bandsaw blades, which permitted more efficient and accurate cutting of construction timber to virtually any size⁴. This development, combined with advances in structural theory and applied engineering, enabled builders to use thinner structural members (such as beams and columns), leading to a more efficient use of logs.

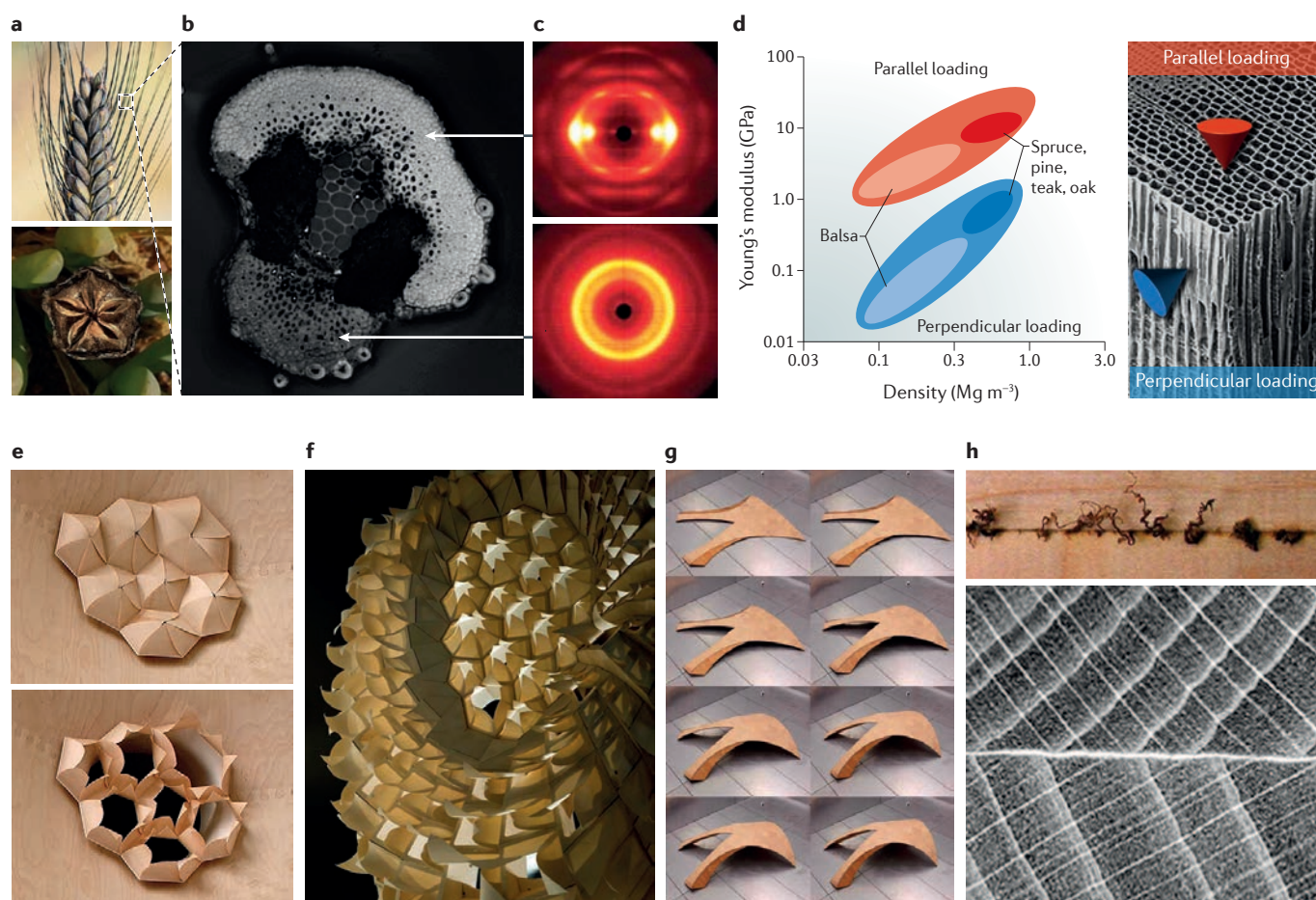


Figure 2 | Properties of wood, as well as architectural and design insights from botanical materials. **a** | Hydro-actuated plant structures, such as wheat awns and the seed capsules of ice plants, can provide valuable design insight into the fabrication of environmentally responsive synthetic systems. Photographs of a living wheat plant seed head with visible awns (top) and a living ice plant with a pentamerous seed capsule in its closed orientation (bottom) are shown. **b,c** | The cross-sectional analysis of a wheat awn reveals the differential ordering of cellulose fibres, confirmed by X-ray diffractions studies. Panel **b** shows an acoustical impedance map of a sectioned wheat awn, revealing local stiffness differences (which vary as a function of image brightness) in the cap and the ridge. Panel **c** shows wide-angle X-ray scattering patterns of the crystalline cellulose at the cap (top) and ridge (bottom), suggesting that the observed differences in stiffness depend on organizational differences of the cellulose fibrils in the two regions. **d–g** | Combining design insight from the structural anisotropy with the directional dependency of the mechanical properties of wood on grain orientation, it is possible to construct humidity-responsive plywood laminates, such as iris-like units, which can be combined to form elaborate multi-component assemblies. This behaviour can be further exploited for the production of large-scale self-expanding deployable shelters that can be transported flat in a potentially cost-effective manner. The left part of panel **d** shows an Ashby plot illustrating the variation in Young's modulus as a function of density for different wood types loaded either parallel (red) or perpendicular (blue) to the grain direction. The plot is accompanied by a scanning electron micrograph (right) of a longitudinally cross-sectioned wood sample to illustrate the different loading directions. Panel **e** shows photographs of closed (top) and open (bottom) radially organized plywood leaflets that actuate as a function of humidity variations. The side of each leaflet measures ~10 cm.

Panel **f** shows a photograph of a clustered mass of humidity-responsive iris-like units that is part of the HygroScope prototype realized by Achim Menges and colleagues. Panel **g** shows a self-erecting model structure composed of cross-ply veneers that transforms from flat to 3D in response to moisture changes. **h** | Inspired by the efficient friction welding of metal structures, new advances in wood joinery are taking advantage of this approach for the production of robust laminates. A photograph of a joint created in seconds through the linear friction welding of two pieces of wood for the production of high-strength bonds without the use of adhesive is shown (top), together with a higher-magnification X-ray photograph of the friction-welded wood joint showing the interface between the assembled units (bottom). The pixel brightness varies as a function of wood density (darker pixels correspond to lower-density wood). Panel **a** (top) is from Albrecht WeiÄer/Getty Stock Image. Panel **a** (bottom) is courtesy of M. Eder and M. Harrington, Max Planck Institute of Colloids and Interfaces, Germany. Panels **b** and **c** are adapted with permission from REF. 24, AAAS. The scanning electron micrograph in panel **d** is courtesy of the N.C. Brown Center for Ultrastructure Studies at SUNY-ESF, Syracuse, NY; the plot is adapted from REF. 115, Cambridge University Press. Panel **e**, HygroSkin — Meterosensitive Pavilion, FRAC Centre Orleans, 2013, is courtesy of Achim Menges in collaboration with Oliver David Krieg and Steffen Reichert, Achim Menges Architect BDA, Institute for Computational Design, University of Stuttgart, Germany. Panel **f**, HygroScope — Meterosensitive Morphology, Permanent Collection of the Centre Pompidou Paris, 2012, is courtesy of Achim Menges in collaboration with Steffen Reichert, Achim Menges Architect BDA, Institute for Computational Design, Transsolar Climate Engineering. Panel **g** is adapted with permission from REF. 27, SAGE. Panel **h** (top) is courtesy of J.M. Leban, INRA, Paris, France. Panel **h** (bottom) is adapted from REF. 116, Taylor & Francis.

However, these more precise shaping technologies and accurate engineering methods required the control of the naturally occurring property variations in wood. One common approach was kiln-drying, an energy-intensive but effective process for limiting dimensional changes in timber caused by changing moisture content. A reproducible, low moisture content was necessary for the introduction of automation into the production process. At the same time, the use of smaller wood elements, such as veneers, flakes or particles, in combination with adhesives became widespread, transforming wood into a modern, predictable material. It was shown that with a decreasing size of wood elements, processing intensity increases and largely replaces labour involvement (capital replaces labour). Moreover, as the size of the wood elements decreases, formability increases and strength decreases, whereas dimensional stability (the degree to which a material maintains its dimensions when temperature and humidity change) and uniformity of mechanical properties improve¹⁰. Recent trends are reversing the tendency to produce engineered wood products from small wood elements by re-introducing solid lumber as a volume-based construction material in the form of cross-laminated timber for structural systems. Cross-laminated timber is used not just in low-rise, but also in high-rise buildings potentially up to 40 stories tall¹¹ that are supported by wall panels up to 35 cm thick.

To meet the growing needs of architectural construction, today's research efforts in the wood sciences are twofold, concentrating on either technical or aesthetic aspects. Technically oriented work is largely pursued by engineers and chemists, with the aim of addressing specific problems, mostly independent of input from designers. Specialists in adhesive chemistry, for example, are continuing to develop resin systems that have desirable structural properties, while eliminating harmful emissions and allowing for wood products to remain biodegradable^{12–15}. Wood connection methods are also being revisited from a materials science perspective. Friction welding of wood (a process adapted from the metal joining industry) shows promise as an option for connections that avoid the pitfalls of stress concentrations and weakening of cross sections resulting from the use of mechanical fasteners, and also avoid the use of adhesives, which limit lumber reuse in an end-of-life scenario^{16,17}. In friction welding, an oscillating movement under pressure produces heat at the interface of two wood elements such that pyrolysis between the organic materials occurs (FIG. 2h). Maintaining pressure during cooling enables the two layers to bond permanently as the softened material hardens into the dark welded interface. The technique is of particular interest for bonding multiple layers of solid lumber in the production of cross-laminated timber panels. The development of this technology is driven by wood's impressive strength-to-weight ratio, low carbon footprint and desirable thermal properties, as well as by the rapid construction speed of large prefabricated wood elements. Despite these advantages, the complexities of wood welding in a production context have so far prevented its widespread adoption.

On the sustainability front, bamboo has been investigated as a fast-growing, potentially ecologically advantageous replacement for conventional wood products, especially in tropical and sub-tropical climates¹². Bamboo's potential is not limited to replacing traditional wood products: it is also being investigated as a fibre reinforcement system for composite materials with bio-based matrices¹⁸. With a specific tensile strength and stiffness similar to that of glass fibre, bamboo has excellent mechanical properties, but its hydrophilic character means that it does not easily blend with hydrophobic polymers¹⁹. These studies point to possible bio-composites that are not only made from renewable materials, but can also exhibit a low or even negative embodied carbon footprint. Additionally, these materials can be designed to quickly decompose, thus solving the end-of-life dilemma of synthetic composites.

Shaping wood has a long history in the building of boats, ships and plywood aeroplanes. In architecture, shaped wood as a structural element has found occasional use in rigid structural shells made from plywood or layered lumber boards nailed and glued together^{20,21}. The emergence of digital 3D modelling tools and numerically controlled fabrication techniques led to the development of a digital process for designing and building wood elements with complex shapes²². In this process, wood-shell design is treated analogously to the design and engineering approach typical for advanced composite materials. Multiple layers of wood veneers can be digitally shaped into structural sandwich elements, and the facing layers consist of multiple layers of kiln-dried wood veneer strips that are cut using computer numerical controlled (CNC) machines according to computational flattening algorithms. The veneer layers are subsequently bonded to CNC-milled structural foam moulds, which are ultimately integrated as the structural core of the sandwich system, minimizing waste. The resulting sandwich shells are dimensionally accurate and stable, with strengths sufficient for elements spanning up to ~25 m.

A second set of efforts are primarily driven by the aesthetic or performative goals of design teams. Several groups have been inspired by wood's hygroscopic (FIG. 2a–c) and orthotropic (that is, the material properties differ along the three mutually orthogonal axes, FIG. 2d) mechanical properties, developing design responses that embrace a behaviour that generations of engineers have attempted to suppress. In nature, the structural anisotropy in the organization of cellulose fibres (FIG. 2b,c) can induce movement through hydration and differential swelling. Examples include the opening and closing of pine cones²³; the soil drilling-like behaviour of wheat awns (FIG. 2a–c), which bend outwards in dry air but straighten in damp conditions so that the grain is eventually pushed into the soil²⁴; and the hinged opening of ice plant seed capsules²⁵ (FIG. 2a). Recent case studies have demonstrated that these design principles can be harnessed for the production of environmentally responsive architectural structures. In a similar manner to the actuating seed dispersive mechanisms described above, macroscale behaviours based on differential swelling can be elicited in plywood bilayers by taking advantage of

the pronounced length changes that can occur in wood, which depend on the direction of the grains.

For example, researchers at the University of Stuttgart produced large-scale prototypes that take advantage of these wood-specific behaviours (FIG. 2e,f). In these structures, the curling of thin, leaf-shaped wood modules changes over time as a function of moisture content (relative humidity)²⁶; the initially flat elements are relatively small (in the 10–20 cm range), and their reversible deformation exhibits reproducible behaviours over several thousand cycles. Using a similar approach, prototypes with sizes up to 1.0 m × 1.5 m that deform from a flat into a doubly curved configuration were also demonstrated²⁷ (FIG. 2g). Quarry workers have long known — going as far back as ancient Egypt²⁸ — that the forces exerted by the expansion of moistened wood can split stone. In efforts to harness this mechanical swelling power, designers have looked into using expanding wood as an actuator for potentially self-assembling modular construction systems^{27,29} and have measured the pressure generated from swelling wood, showing that it can be as high as 91 MPa. Theoretical values are even higher.

Wood has not been left out of the current interest in 3D printing, but the use of wood fibres has been challenging because most printers rely on highly controlled material properties for consistent results. Combining cellulose fibres (~40%) with a polymer can produce an extrudable source filament that has some of the same hygroscopic properties as wood, but retains the printability from its thermoplastic polymer fraction³⁰. Researchers at the Massachusetts Institute of Technology and at the University of Stuttgart have investigated how multimaterial fused filament fabrication printing of these cellulose-based filaments can produce shapes that fold or curve upon changes in moisture content, without the need for direct external actuation³⁰. This process involves the production of bilayer structures using a swellable cellulose-based filament in conjunction with a second non-swellable layer, such that differential swelling leads to a change in the overall geometry.

Ceramics

Ceramics (FIG. 3) were the first material ever created by humans when, through the simple act of firing clay, this soft matter was transformed into a durable, crystalline material. The slow but steady advances realized over approximately 30,000 years have recently accelerated owing to the implementation of precision processes for the preparation of raw materials, enabling production lines and computer-controlled kilns to output tiles with highly consistent quality and small production tolerances³¹. Chemistry and materials science have contributed to producing an ever expanding range of glaze finishes that exhibit almost any possible colour and effect, including the photorealistic mimicking of naturally occurring material patterns obtained through digital inkjet printing³¹. In addition, modern advances in high-resolution materials characterization (FIG. 3a–d) have permitted an unprecedented understanding of crystal nucleation and growth processes, as well as fracture behaviours in bulk ceramic materials. In terms of digital control and design,

the ancient art of ceramic mosaic production has been automated and streamlined through the incorporation of digital image processing and pick-and-place robotic arms for the high-throughput assembly of large-scale mosaics that would have previously been cost prohibitive³².

The well-established clay-bodies and firing strategies that led to more or less vitreous ceramic products have been recently expanded through foaming processes developed by artists working collaboratively with the European Ceramic Work Centre³³. Compared with conventional clay-based ceramics, these clay bodies are relatively low in kaolinite (5–25%) but high in alkali salts and alkaline earth metal salts (10–30%) and frits (40–75%); they are being developed for both artistic purposes and to reduce the carbon footprint of ceramic facade elements³⁴. Other porous porcelain elements have been produced by burning out inflammable additives from the clay body during kiln firing. The ability to produce tortuous perforations at the sub-millimetre scale results in materials with sound absorption coefficients in the range of 0.25–0.6 (frequency dependent) for samples that are only 12 mm thick (FIG. 3e). By increasing the thickness, commercially viable absorption rates can be achieved. Micrometre-scale porosity in fired ceramic elements has also been used to achieve the absorption and release of moisture; this effect has been exploited to design evaporative cooling facades for both research pavilions and tall commercial buildings³¹ (FIG. 3f).

Although ceramic 3D printing is a rapidly evolving technology, it has not yet advanced enough to integrate into commercial production. Ongoing research in this area involves materials scientists, chemists, software and robotic specialists, as well as designers³⁵. A common ceramic 3D printing method consists of the nozzle-based extrusion of a small bead of moist clay over multiple layers or over a configurable mould^{36,37}. This technique is an adaptation of the fused filament fabrication modelling approach to clay materials. An alternative method is binder-jetting, whereby a thin layer of ceramic powder is solidified with an adhesive binder through a process similar to ink-jet printing, and the resulting part is built up in a layer-by-layer fashion³⁸ (FIG. 3g). The binder-jetting process produces a fairly smooth surface that can be glazed, whereas extrusion methods result in a slightly scalloped surface texture (FIG. 3h). Binder jetting is more precise, but also slower than extrusion-based methods. As with all 3D printing processes, the material composition and the related deposition strategy lead to design constraints, such as limitations in terms of overhangs and undercuts. The firing strategies add another means to influence the quality of the output: higher kiln temperatures in combination with higher-quality clay bodies lead to more vitrified and thus stronger, more durable finished products.

Metals

Metals (FIG. 4) followed ceramics in the history of man-made materials — ceramic kilns gave rise to the smelting of copper and iron into bronze³¹. Alloy development contributed significantly to advances in building and infrastructure construction, but also had strategic importance for weapons and armoury. Metallurgists were the first

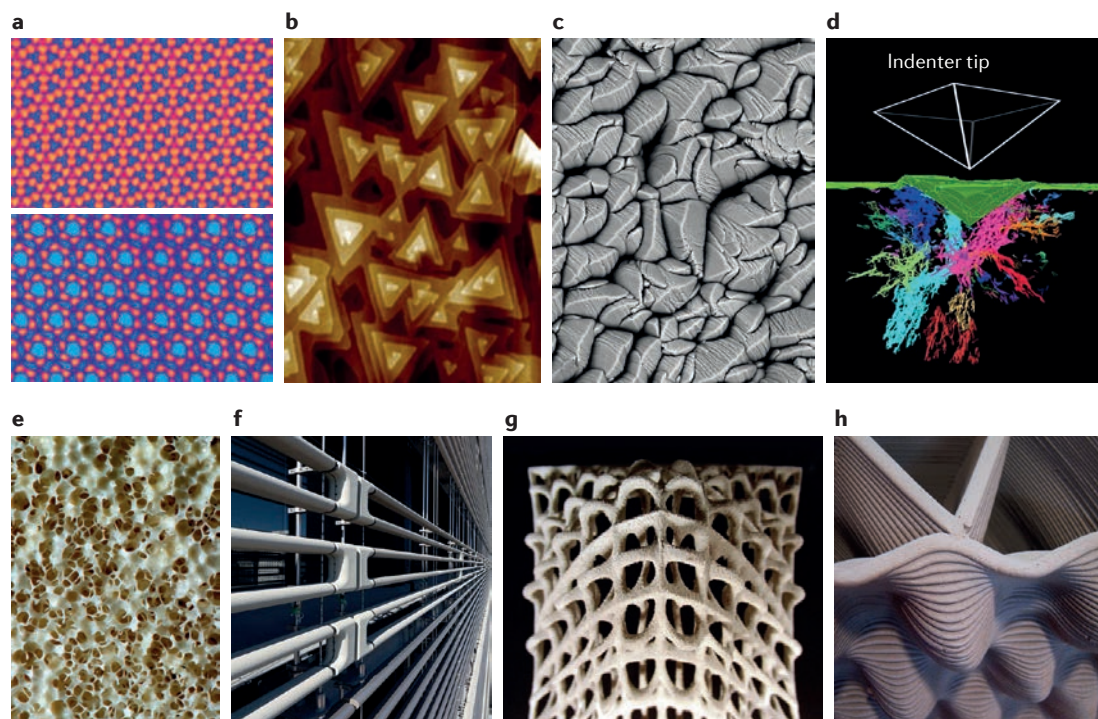


Figure 3 | Ceramic characterization and production from the nanoscale to the macroscale. a–d | From the atomic-level characterization of ceramic polymorphs and the studies of nano- and microscale crystal nucleation and growth processes to the 3D characterization of damage zones in fractured ceramics, modern advances in materials science are providing new design guidelines for the fabrication of their macroscale analogues. Panel **a** shows the atomic structure of the α (upper) and β (lower) phases of silicon nitride as revealed by aberration-corrected revolving scanning transmission electron microscopy¹¹⁷ (in this false-coloured micrograph, columns of silicon atoms are indicated in orange; the field width of each image is 3.5 nm). Panel **b** shows an atomic force micrograph of a series of propagating triangular screw dislocations on the surface of bismuth selenide (field width: 1 μm). Panel **c** shows a scanning electron micrograph of the growth front of a high-temperature yttria-stabilized zirconia thermal barrier coating for applications in aerospace gas turbines (field width: 75 μm). Panel **d** shows a micro-computed tomographic 3D reconstruction of subsurface damage arising from nanoindentation in Syalon 101 silicon nitride (field width: 20 μm). **e–h** | A more detailed understanding of these hierarchical structure–function relationships in ceramic materials can be used for mechanical optimization in applications ranging from microstructured porous ceramics for sound absorption and evaporation-driven whole-building cooling to the 3D printing of larger lightweight support structures and custom 3D-printed ceramic modules. Panel **e** shows a photograph of a porous ceramic panel (pore size ~ 0.8 mm) produced by soaking polymer foam in a ceramic slip. During kiln firing, the foam burns out, leaving a tortuous porous material behind. Panel **f** shows a photograph of the porous ceramic evaporative cooling elements on the facade of the Sony City Osaki building in Tokyo. Panel **g** shows a photograph of a 3D-printed ceramic scaffold produced through the chemical binding of mineral particles. Panel **h** shows the extrusion-based 3D printing of wet clay; the geometry of this structure is designed to optimize the effects of thermal mass (the ability of a material to absorb and store heat) in naturally ventilated spaces, which helps in maintaining a stable temperature. Panel **a** is courtesy of J. M. LeBeau, North Carolina State University, USA. Panel **b** is adapted with permission from REF. 118, Penn State University. Panel **c** is courtesy of J. C. Weaver and D. R. Clarke, Harvard University, USA. Panel **d** is courtesy of K. O’Kelly, Trinity College Dublin, Ireland. Panel **e** is courtesy of S. Mhatre, Harvard University, USA. Panel **f** is courtesy of T. Yamanashi, Nikken Sekkei Ltd., Japan. Panel **g** is courtesy of R. Rael, Rael San Fratello, USA. Panel **h** is courtesy of P. Gómez-Tena, Instituto de Tecnología Cerámica, Spain.

materials scientists. The structural use of cast and later wrought iron was an initial response to the fire hazards of textile mills of the early industrial age in 18th century England⁴. The limited tensile strength of the material, however, severely constrained the maximum spans of beams, whereas its strength in compression still favoured its use in funicular arches and vaults reminiscent of much older brick and stone construction. It was the development of low-carbon steel production and the associated advances in tensile strength, plasticity and stiffness that finally enabled the larger horizontal spans

and slender steel-frame buildings that shape today’s cities and their infrastructure. In recent years, the ability to directly investigate and simulate grain growth processes and stress responses, in conjunction with ultrahigh resolution 3D imaging of chemical gradients across phase boundaries (FIG. 4a–c) are providing an exciting trajectory for the development of new high-performance alloys for novel applications. As a result, new metal alloys and 3D printing approaches have recently become of interest to designers wishing to advance their craft through materials explorations.

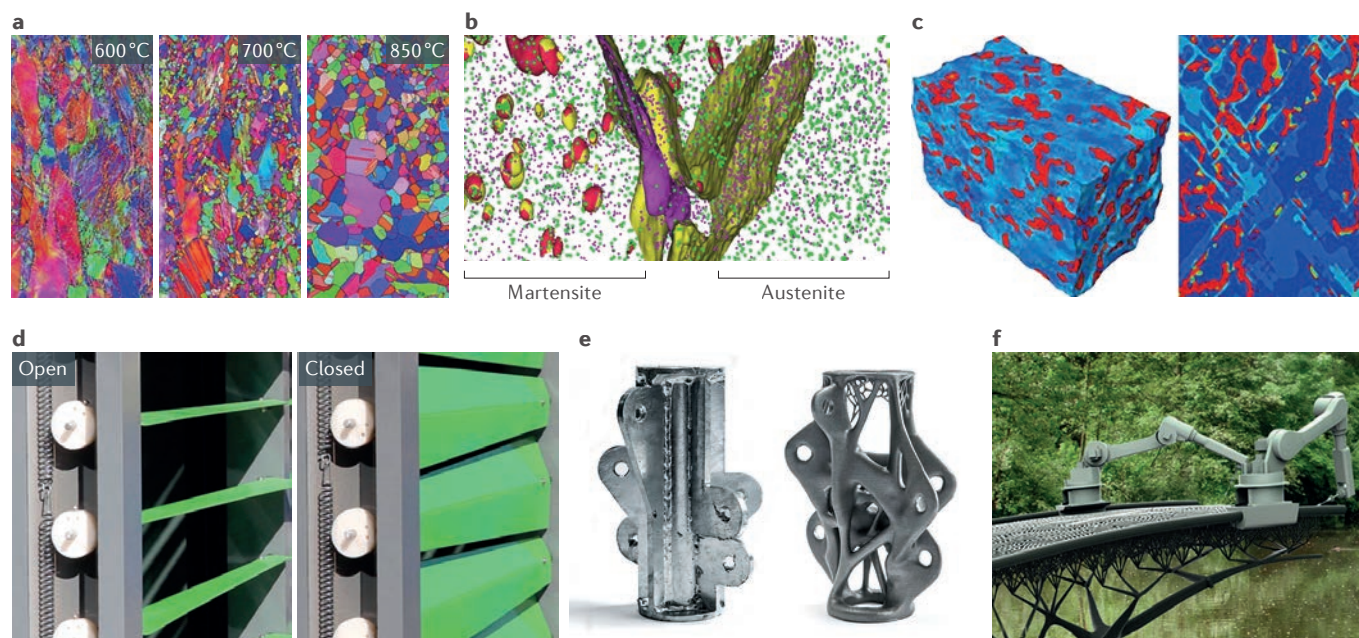


Figure 4 | Modern advances in metal structural characterization and architectural applications. a–c | From monitoring grain growth to the 3D mapping of chemical gradients across phase boundaries and the use of finite element simulations for investigating stress responses in multiphase steels, materials science approaches can be implemented for investigating the performance of metals for use in non-traditional applications. Panel **a** shows representative inverse pole figure maps generated from electron backscatter diffraction data acquired from 600, 700 and 850 °C partially recrystallized, cold-rolled twinning-induced plasticity (TWIP) steel showing grain growth during annealing. Panel **b** shows a 3D reconstruction of atom probe tomography data, revealing chemical gradients across phase boundaries between the martensite and austenite phases in transformation-induced plasticity (TRIP) steel. Manganese atoms are shown in purple and nickel atoms in yellow; 18 at.% manganese isosurfaces are shown in green, 12 at.% nickel isosurfaces in red (where at.% is atomic percent). Panel **c** shows stress contours in 3D (left) and 2D (right) representative volume elements of DP600 steel containing 20% martensite. High stresses (denoted in red) of up to 1.7 GPa are observed in the martensitic zones. **d–f** | Architectural applications of metals include the incorporation of shape-memory metals in adaptive facades, the 3D laser sintering of metal powders for the economical production of topology-optimized nodes, and robotically welded bridges. Panel **d** shows a photograph of a thermally actuable adaptive facade using shape-memory metals. Panel **e** shows photographs comparing traditional structural steel nodes (left) with topology-optimized geometries (right) produced through the selective laser sintering of metal particles. Panel **f** shows the rendering of a 3D-printed bridge that will be fabricated using a multi-axis industrial robotic arm with an integrated welding head for the *in situ* production of robust metal structures of arbitrary geometries. Panel **a** is adapted with permission from REF. 119, Springer. Panel **b** is adapted with permission from REF. 120, Elsevier. Panel **c** is adapted with permission from REF. 121, Elsevier. Panel **d** is courtesy of J. Grinham, Harvard University, USA. Panel **e** is courtesy of Arup and D. De Jong, David fotografie, Amsterdam, the Netherlands. Panel **f** is courtesy of MX3D, Amsterdam, the Netherlands.

For example, shape-memory alloys — materials that feature reversible transformations between two crystalline phases (austenite and martensite) upon heating — have long attracted designers for the actuation of kinetic facades and other structures. Work on building applications has produced several successful prototypes that deploy shape-memory alloys to automate elements, without the need for power or external actuators, for shading and light control³⁹ (FIG. 4d). For seismic retrofits, shape-memory alloys are of interest because of their ability to elastically recover large strains on the order of 6–10%. When used as reinforcement elements, systems based on shape-memory alloys can be engineered to pre-stress historic masonry structures such that pre-stressing loads are minimal during normal loading, while avoiding major cracks and failure during a seismic event⁴⁰.

Until recently, 3D printing of structural metal seemed out of reach for architectural applications, and generally it

remains a slow and costly procedure. The most common methods are selective laser sintering and electron-beam melting, which can fuse metal particles into fully sintered, functional parts, albeit within a limited build size. In addition, different metals can be combined into functionally graded parts. The technology remains slow and is usually too costly for architectural applications. Nevertheless, engineers at Arup have explored its use for the production of lightweight structural steel nodes, using computational topology optimization techniques to maximize the strength- and stiffness-to-weight ratios⁴¹ (FIG. 4e). Although the resulting nodes have been shown to reduce material consumption while maintaining stiffness and strength⁴¹ compared with conventionally built connections, cost considerations remain a major obstacle for their use in construction.

Smaller architectural prototypes have been produced using systems whereby metal particles are deposited

along a build path, often involving an industrial robot for motion control. The idea originated in a 1925 patent by Ralph Baker⁴²; in its modern adaptation, the particles are immediately laser-fused into free-form parts⁴³. Related to this technique, but fundamentally different from a materials perspective, is direct ink writing, whereby a metal ink is annealed using lasers. The technology is currently geared towards electronics and related small-scale systems⁴⁴: direct metal ink writing produces conductive 2D or 3D metal structures, with the goal of printing electronics and their surrounding encapsulation in a single process. Building applications, such as 3D-printed electrical wiring for communication and use in other printed building components, are conceivable, but have not yet been attempted.

Researchers have also combined welding machines with robotic arms to create free-form curvilinear surface forms and branching metal networks, fundamentally extending well-established robotic welding into a freeform-fabrication technology. Molten metal is solidified as it exits the nozzle, thus eliminating the need for support structures, although initially only small objects have been produced^{45,46}. An interdisciplinary team in the Netherlands, MX3D, led by designer Joris Laarman, has recently scaled up the technology for the production of sculptures, furniture and a small bridge designed to span a canal in Amsterdam (FIG. 4f). This effort has added little in terms of materials technology, but instead focused on implementing robust design-to-production workflows and reliable, repeatable physical outcomes. The technology uses steel, stainless steel, bronze or copper.

Concrete

Research on concrete (FIG. 5) has relied heavily on the collaboration of designers and engineers with chemists and materials scientists. The appeal of the material lies in its ease of formability in the wet state and its strength, durability and fire-resistance in the hardened state, similar in many ways to clay-based ceramics. The early development of reinforced concrete was driven by the need to provide fire-resistant structural systems for production spaces of the emerging industrial age, overcoming the limitations of heavy timber and metal structures. Following the invention of Portland cement by Joseph Aspdin, an English bricklayer, in 1824, the first patents on reinforced concrete were filed in the middle of the 19th century by Joseph-Louis Lambot and Joseph Monier in France, without however considering applications in buildings⁴⁷. This pioneering work was soon followed by the development of engineering solutions such as horizontal spanning systems for buildings⁴⁸. The compressive strength of these early concrete materials (10–15 MPa) was less than 10% of what is possible today.

The following development of concrete in the 20th century is a good example of how only the combined contributions from the fields of materials science and structural engineering could bring about a material system of practical use for construction. Structural engineering needed accurate numerical models for predicting the interaction between reinforcing steel and concrete in a single structural element, while materials

experts developed better cements and eventually admixtures. In 2000, ~15% of the total concrete used worldwide contained additives⁴⁹. What is less known to building professionals is that many concrete additives are derived from natural materials — plasticizer, for example, is commonly produced from lignin, a biopolymer sourced from wood⁴⁹.

In the past 20 years, research has advanced the mechanical properties of concrete by optimizing the granularity of the material structure and by devising new superplasticizers and admixtures. More recently, this work has included research on additives from the domain of nanomaterials, such as carbon nanotubes⁵⁰ (FIG. 5a). In addition, modern characterization approaches, including high-resolution elemental and phase mapping, as well as high-throughput computed tomography (FIG. 5b–d), have become powerful tools for the optimization of concrete formulations. Short metal and other fibres can now partially replace traditional steel or pultruded fibreglass reinforcement bars when combined with new cements and admixtures, resulting in ultrahigh performance fibre-reinforced concrete (UHPFRC). These materials reach compressive strengths of 280 MPa in practice, and over 800 MPa under laboratory conditions where steam curing and pressure treatments can be applied^{51,52}. The extremely high strength-to-density ratio of these new materials allows for the use of thinner members than were previously thought possible with concrete. Designers are enjoying a new interest in shaping structures from the furniture to the infrastructure scale through the incorporation of these extremely thin, yet structural, concrete elements.

This new concrete architecture, however, requires innovative reinforcement systems because the embedded fibres do not generate enough tensile and bending strength for all applications. The extreme thinness of structural members leaves no room for traditional steel reinforcement bars that may be larger in diameter than the actual member cross sections. Reinforcement textiles made from glass or carbon fibres have been used to enhance the bending capacity of UHPFRC structures. Post-tensioning of UHPFRC is also being investigated as a means to extend the load-bearing capacity of high-performance concrete in bending⁵³. Sand-covered carbon lamellae have been demonstrated as post-tension members. Such carbon reinforcement systems show high tensile strength that combines well with the superior mechanical properties of UHPFRC.

This high-performance material also requires more precise construction methods, because construction tolerances for conventional concrete construction are too large for thin UHPFRC elements. Formwork costs have long been a major impediment for more imaginative and efficient use of reinforced concrete. Even for simple orthogonal skeletal frames, the formwork cost is often in the range of 35–60% of the total construction cost⁵⁴. Pre-casting normally reduces on-site construction time and cost, but the cost of precision formwork for UHPFRC elements is likely to remain relatively high. As modern architecture requires the fabrication of increasingly complex geometries, several approaches have emerged to address the high cost of formwork.

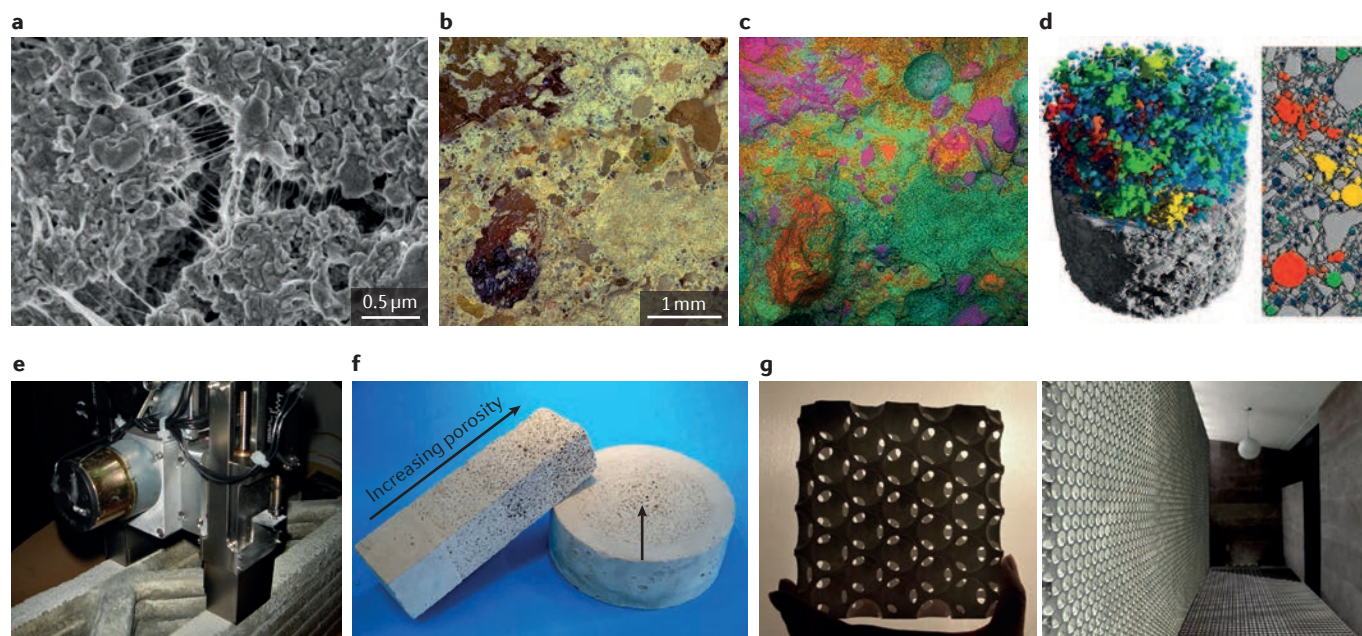


Figure 5 | Recent advances in concrete characterization and fabrication. a–d | By combining large-area correlative optical microscopy and elemental mapping with 3D X-ray tomography, new insights into failure modes can be achieved, which enables the structural optimization of concrete-based hybrid materials. Panel **a** shows a scanning electron micrograph depicting crack bridging in a single-walled carbon nanotube–cement composite with bridging nanotube bundles (field width: 2.5 μm). Panel **b** shows an optical micrograph of a 4 mm \times 4 mm section of a fractured concrete wall showing the compositional heterogeneity that characterizes this class of materials. Panel **c** shows an energy-dispersive spectroscopy elemental map of the same 4 mm \times 4 mm region, showing the elemental distribution of the different phases in this material: aluminium, orange; silicon, magenta; calcium, green; iron, yellow. Panel **d** shows a colour-coded 3D tomographic reconstruction (accompanied by a 2D slice) of the pore size distribution in an expanded perlite-containing cylindrical concrete sample measuring ~ 0.75 cm in diameter. **e–g** | Modern architectural concrete formulations for the production of 3D printable buildings, monolithic forms with functionally graded porosity and ‘breathable’ macroporous walls can be customized for specific load-bearing applications. Panel **e** shows extrusion-based concrete 3D printing for the generation of architectural-scale structures. Panel **f** shows samples of functionally graded concrete with tunable linear or radially organized porosities. Panel **g** shows highly ordered macroporous panels created by casting concrete in a 3D-printed mould filled with hydrogel spheres. Once the concrete has cured and the spheres have lost some of their initial volume, they can be easily removed. Panel **a** is adapted from REF. 50 under a Creative Commons license [CC BY 3.0](#). Panels **b** and **c** are courtesy of J. C. Weaver, Harvard University, and A. Masic, Massachusetts Institute of Technology (MIT), USA. Panel **d** is adapted with permission from REF. 122, Elsevier. Panel **e** is courtesy of B. Khoshnevis, Contour Crafting Corporation, USA. Panel **f** is courtesy of S. Keating, MIT, USA; the samples were created by S. Keating and N. Oxman (Mediated Matter, MIT Media Lab) in collaboration with T. Cooke and J. Fernández (MIT Building Technology Department). Panel **g** is courtesy of Z. Liao, Hong Kong, China.

A design and engineering team at the Graz University of Technology, for example, is developing adaptive formwork systems for the construction of doubly curved thin UHPFRC elements⁵⁵. A robotic manipulator configures a pin-based formwork that is used to generate a form of a desired geometry, which can then be used to cast precision concrete segments for doubly curved shells. Edges are robotically ground to tolerances in the 0.5 mm range to allow for dry connection with newly developed bolting systems that are much like those used in steel construction.

A second effort that addresses formwork costs has focused on the development of foldable systems. Casting flat concrete plates in a factory context is relatively cost effective and can be largely automated⁵⁶. Origami-inspired approaches that take advantage of the cost and quality benefits of producing flat slabs, delegating the creation of spatial forms to the assembly or installation

process, have been demonstrated. The method first proved effective for the production of a concrete canoe⁵⁷, but prototypical architectural structures have also been produced⁵⁸. This modern approach involves the computational design and engineering of thin concrete folded plate systems as folded structures that can be flattened into production-ready 2D patterns. The need to fold adjacent plates is accommodated through the integration of carbon-fibre reinforcement mats that bridge the folds. The fold lines are left free of cementitious matrix during the casting process, so that a living hinge is produced, and, as a result, the required scaffolding is much simpler than traditional formwork. However, this technique requires a detailed understanding of the behaviour of the carbon reinforcement meshes during bending in the folding process, as well as their complete and structural encapsulation with specialized non-shrinkage structural grouts after the folding is complete.

A third advance has been the development of extrusion methods for structural elements with hollow cross sections^{59,60}. Fast-curing concrete mixes are pushed through a forming die to produce thin-walled shapes that harden immediately after exiting the die. In an alternative approach (which borrows principles from the slip-forming of structural cores in high-rise construction), curved and twisted concrete columns can be created using an industrial six-axis robot that moves a short formwork tube up at the same speed at which a curing concrete mix is slowly lowered through it⁶¹. During the pouring process, the lifting and deposition speeds are adjusted based on the continuous monitoring of the stiffness of the wet mix with a penetrometer. The data are processed in real time such that the robotic actuator advances the tube whenever the concrete–fibre mix has set enough to provide the strength needed for pouring the next layer. Tilting the tube enables curved forms to be created; thus, the concrete mix needs to have high early strength and short curing times, yet it needs to remain workable long enough to not clog the extruder.

A fourth approach has been the adoption of 3D printing in concrete construction; this typically involves expertise in the fields of concrete rheology and chemistry, as well as in mechanical and civil engineering. A first study in 1997 proposed (but failed to patent) a technology whereby thin layers of concrete are deposited and then selectively solidified through a nozzle deposition system⁶². Enrico Dini was the first to publish and patent a development of this approach, essentially scaling up binder jetting 3D printing to a construction scale^{63,64}. Instead of using the traditional single ink-jet nozzle common in binder jetting, Dini's system involves multiple closely spaced nozzles, mounted on a moving gantry, to more rapidly solidify the compacted powder where desired. After curing, the labour-intensive post-processing involves 'excavating' the hardened parts from the surrounding powder on the machine bed.

An alternative technology — contour crafting — was developed by researchers at the University of Southern California starting in the late 1990s. Inspired by 3D printing based on fused filament fabrication, a delivery system and nozzle deposits a wet cement matrix as it moves via a gantry-like mechanical frame^{65–67}. This concrete deposition system incorporates a trowel-like mechanism attached to the print head that leaves a smooth finish on the otherwise scalloped concrete surface (FIG. 5e). Other approaches have embraced the inherently scalloped morphology of 3D-printed concrete as a design element or rely on secondary smoothing processes to eliminate these inherent surface irregularities. The main motivation for the development of these printing technologies was the desire to develop rapid and fully customizable on-site construction and the simplification of construction logistics. Later research at the University of Loughborough used a similar approach^{68–70} with a focus on pre-fabrication. In the following, we refer to contour crafting and the work at Loughborough as 'extrusion-based approaches'.

From a materials science perspective, the main challenge for extrusion-based approaches is to optimize the properties of the wet concrete to enable controlled

deposition of the material without the use of external formwork, providing at the same time excellent mechanical properties and durability for the cured material. An optimum mixture for extruded concrete is based on a 3:2 sand-to-binder ratio, 1% superplasticizer and 1.2 kg m⁻³ 12/0.18 mm (length/diameter) polypropylene fibres⁶⁸. The mix extrudes well through a 9 mm nozzle and is stiff and strong enough to support up to 61 layers in a single printing session. The mix has a water-to-cement ratio of 0.26 and a compressive strength (at 28 days) of 110 MPa. The properties of the hardened mix are similar to those found in conventionally placed concrete, with a slightly higher density and a greater variability in compressive strength⁷¹. Mechanical properties, however, are not isotropic, and microscopic imaging revealed a parallel orthotropic microstructure resulting from the layered material deposition process⁷².

Both concrete extrusion-based technologies are currently being investigated for lunar construction. During the 1994 Endeavour mission, a small concrete sample was successfully mixed and produced in space and then brought back for analysis⁶⁶. Current plans for lunar construction might involve an extrusion-based printing approach that uses lunar regolith as a base material, bonded with a binder provided from Earth⁶⁴. Mechanical and process testing has confirmed that lunar regolith can be 3D printed into a functional structural material.

In parallel to the development of concrete 3D printing, there is ongoing research on new concrete additives to reduce the carbon emissions resulting from Portland cement production. Fly ash, a by-product of steel production, can be substituted for 15–30% of Portland cement⁴⁷, resulting in a reduction in embodied carbon footprint as a function of fly-ash fraction⁷³. A related research effort seeks to develop lightweight concrete with reduced thermal conductivity and to minimize cement consumption while maintaining appropriate compressive strengths^{74–76}. Porous aggregates, alumina-based foaming agents and aerogels are being investigated for these applications; these new concrete mixes are either placed conventionally or sprayed onto flat formwork in a layer-based approach similar to lamination strategies used for composites. Spraying concrete also enables control over the deposition of porous mixes when insulation properties are more important than compressive strength. This is a step towards developing functionally graded concrete systems that feature varying porosities and densities to reduce material consumption and minimize deadweight, which have been successfully demonstrated (FIG. 5f).

Previous research efforts on the creation of porous concrete have primarily focused on weight reduction and increased material usage efficiency, but more design-driven approaches are now being considered for large-scale applications. One example is the production of highly ordered large-scale porosity effects, which can be achieved through the incorporation of hydrogel spheres in combination with customized formwork systems (FIG. 5g). In this approach, hydrogel spheres are expanded with water and used to create hollow voids in concrete panels. After drying, the hydrogel spheres can be easily removed, enabling the production of highly ordered and

periodic perforated concrete panels. The resulting panels show novel ornamental effects, and can act as privacy screens and sun-shading devices.

Glass

Silica glasses, unlike their crystalline analogue, quartz, are characteristically amorphous (FIG. 6a), and owing to their optical transparency and ease of processability, they have been in continued use for more than 5,000 years. Gold nanoparticles in medieval stained-glass windows are often cited as the first architectural use of nanotechnology⁶. Historically, glass was considered a precious material to be used only sparingly in buildings.

Advances in glass chemistry and in glass processing technology coincided with the Modern Movement embracing transparency in the 1920s and with the desire to blur the distinction between the interior and exterior in buildings. However, the increasingly large expanses of glass created problems of heat loss in cold climates, solar gains in warm climates and the need for glare control to maintain productive work environments. To meet these demands, multilayered glazing systems with gas or polymer-film infills replaced inefficient single-pane windows. Coatings such as silver films are used on low-emissivity glass to reduce infrared transmission while letting visible light through.

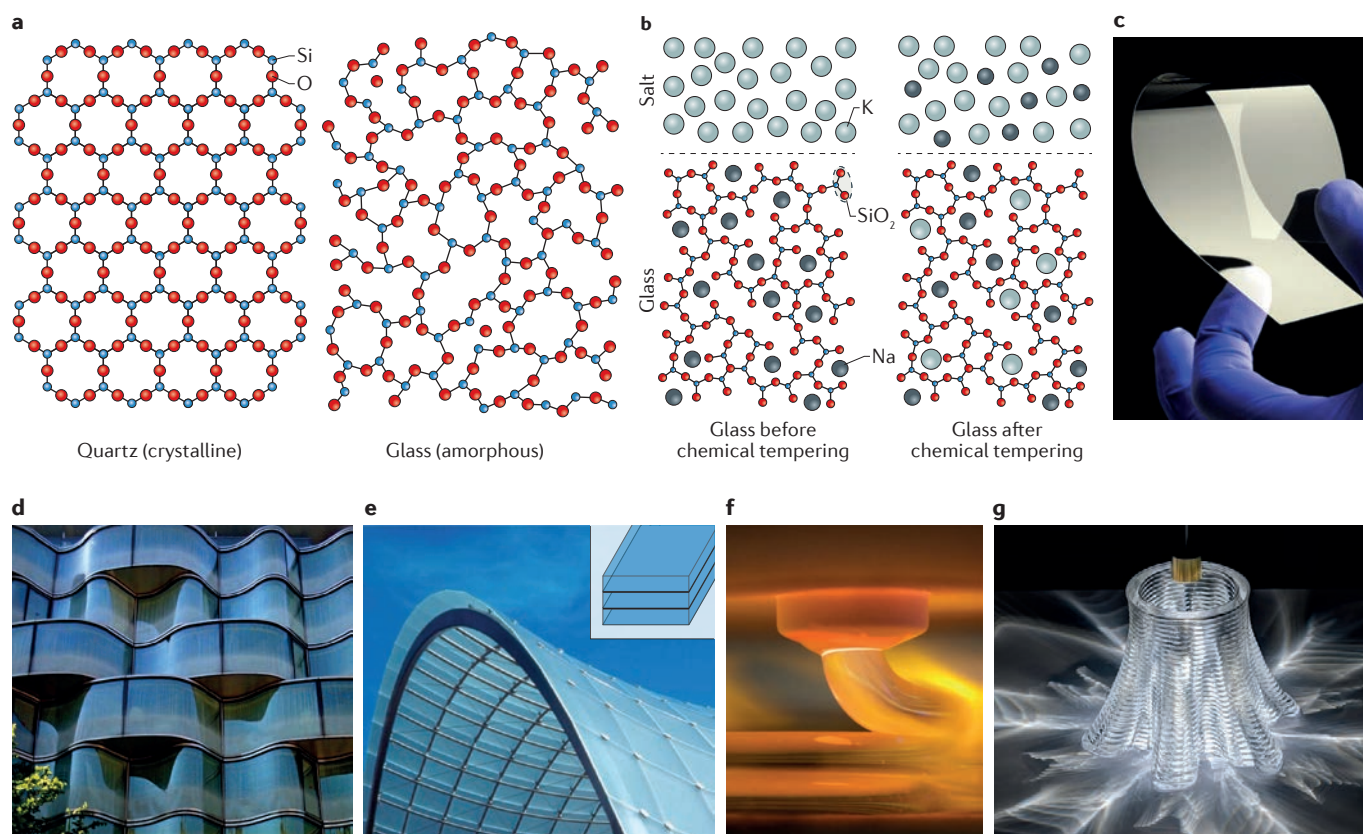


Figure 6 | Glass processing and architectural applications. a–c | Taking advantage of the intrinsically disordered molecular structure of glass, and through the use of chemical tempering processes, it is possible to create toughened glass for a wide range of technological applications. Panel **a** shows a schematic illustrating the structural differences between quartz and glass. Panel **b** shows a schematic depicting the process of glass chemical tempering. When glass is submersed in a potassium salt bath at 300 °C, the sodium ions in the glass surface are exchanged with potassium ions from the surrounding media. As the potassium ions are larger than the sodium ions, this ionic substitution induces a compressive state in the glass surface, substantially strengthening the material. Panel **c** shows an image of high-strength chemically tempered glass; this glass is commonly used for display applications in which fracture resistance is a key factor. **d–g** | Toughening of architectural-scale glass structures can involve the chemical tempering of large curved glass panes or the production of laminated glass composites for tiled curtain walls. In addition, recent developments in glass 3D printing technology now enable the rapid production of optically transparent architectural forms of complex and fully customizable geometries. Panel **d** shows a photograph of a chemically tempered curved glass facade. Panel **e** shows a photograph of laminated glass panels (in the inset, glass is indicated in blue and polymeric interlayers in black) that constitute a curtain wall facade. Panel **f** shows a photograph of molten glass emerging from the nozzle of a 3D printer. Panel **g** shows an example of a representative form made possible with this approach. Because of its optical transparency and layered structure, complex caustic lighting effects can be created when this object is illuminated from above with a point light source. Panel **c** is courtesy of Corning Inc., USA. Panel **d** is from Google Street View, © 2017 Google. Panel **e** is courtesy of B. Gulick and James Carpenter Design Associates Inc., USA. Panel **f** is courtesy of S. Keating, Massachusetts Institute of Technology, USA. Panel **g** is courtesy of A. Ryan, Lexington, Massachusetts, USA.

Adaptive glazing solutions have been developed to respond to the dynamically changing environmental and programmatic needs of glazed envelopes or interior glazed partitions. Various technologies, such as liquid-crystal films with tunable opacity and chromogenic materials, have been commercialized, but they normally come at a substantial supplementary cost. More recently, structural colour effects have shown promise for the control of light transmission and privacy, but more research is needed to develop scalable, robust application systems that can withstand the challenges of building applications. In addition, thin-film interlayers that could be potentially combined with glazing systems to produce optical adaptability over short time intervals have been developed^{77,78}.

Thermally induced pre-stressing led to more structurally sound glass; this, combined with advances in processing technology, allowed for large glazing systems for facades and structural glass beams or columns for buildings. Thermal tempering can be routinely used to strengthen planar geometries, but it is challenging to implement when working with complex forms. To mitigate these issues, chemical tempering (FIG. 6b) has become more widely used, for example, for the production of thin films for display applications (FIG. 6c) and of free-form architectural facades (FIG. 6d). In this process, an ion-exchange reaction replaces sodium ions (which are normally present in a substantial amount in commercial glasses) in the glass structure with larger potassium ions, creating a pre-stressed condition. Borrowing design principles from the composites industry, laminated glasses (FIG. 6e) have been demonstrated to exhibit remarkable damage tolerance under complex loading regimes while simultaneously providing additional design freedom, and are now common place in architectural settings.

For the production of more complex geometries, 3D printing of glass has been successfully demonstrated with a range of techniques, including binder jetting and selective sintering. However, historically the outputs from these processes were of limited architectural value because of their fragility and optical scattering properties that appreciably increased their visual opacity⁷⁹. Building on these previous efforts, optically clear glass has been recently 3D printed (FIG. 6f,g) through a high-temperature extrusion process, conceptually similar to that used in polymer-based fused filament fabrication printers⁸⁰. Owing to the complexity of such an endeavour, the large interdisciplinary team included computational designers, structural and mechanical engineers, glass scientists and process control specialists. During the construction of this 3D printing system, particular attention was paid to thermal management issues in relation to glass viscosity, deposition rate, layer height and post-printing mechanical stability, all of which had a direct effect on the diversity of printable forms and on the reduction of residual stresses in the final product.

Synthetic composites

The advances in polymer development in the 1910s led to their first applications in buildings in the 1950s, with structural engineers quickly embracing glass fibre-based reinforcement strategies. Dome-shaped

enclosures for military applications made from glass-fibre-reinforced panels protected radar equipment from exposure to the elements without affecting the transmission of electromagnetic radiation. Following these early successes, architects briefly embraced 'plastic' as a material that offered seemingly unlimited design freedom. Early attempts at producing polymer sandwich modules for dwellings and facades were met with initial enthusiasm, but this excitement tapered off quickly after a series of technical problems and failures raised awareness regarding their limited UV resistance and long-term durability.

Today, the use of composites in architecture remains in its infancy in comparison with their widespread use in the automotive, marine and aerospace industries. This is largely due to the general lack of codified structural engineering standards for buildings or infrastructure made of composite materials, and the need to prove that fire-resistance and flammability requirements can be met. Although there have been steady advances in terms of materials development, such as the integration of carbon fibre to maximize strength-to-weight ratios, measurable advantages in the building context in terms of cost effectiveness still have to be demonstrated. Despite these shortcomings, there has been some progress in the more widespread use of composites in an architectural context. These include the production of a new generation of thermoset resins and coatings to control flammability, which have enabled the use of glass-fibre-reinforced panels as lightweight cladding solutions for buildings⁸¹. In addition, pultruded fibre-glass structural profiles are finding more common use in windows and in structural applications, such as bridges or agricultural buildings, where aggressive air quality would quickly corrode steel⁸². From a sustainability perspective, despite the energy-intensive methods for the production of resins and fibres, the embodied environmental impact of composite materials is, surprisingly, relatively low; this is because glass-fibre-reinforced panel systems use relatively low quantities of material to achieve a good performance metric, which results in a simultaneous reduction in energy use and carbon emissions during production. Advances in the characterization and processing of composite materials are providing new insights into their properties and their applicability in a building context (FIG. 7a–c).

The biggest drawback of fibre-reinforced composites remains the lack of end-of-life solutions other than landfilling or incineration. One response has been to develop materials systems based on natural fibres such as hemp, jute, sisal or coconut coir and biodegradable resins that are often starch- or cellulose-based^{83,84}. However, many natural fibres are hydrophilic, which limits their ability to bond to various biodegradable matrix materials, triggering a search for biodegradable coupling agents⁸⁵.

In contrast to the beam-like structural elements discussed above, a highly developed use of composites is as structural membranes for tensile roof structures. In this context, fibreglass or polyvinyl chloride (PVC) woven fabrics are used extensively, coated with PTFE (Teflon)

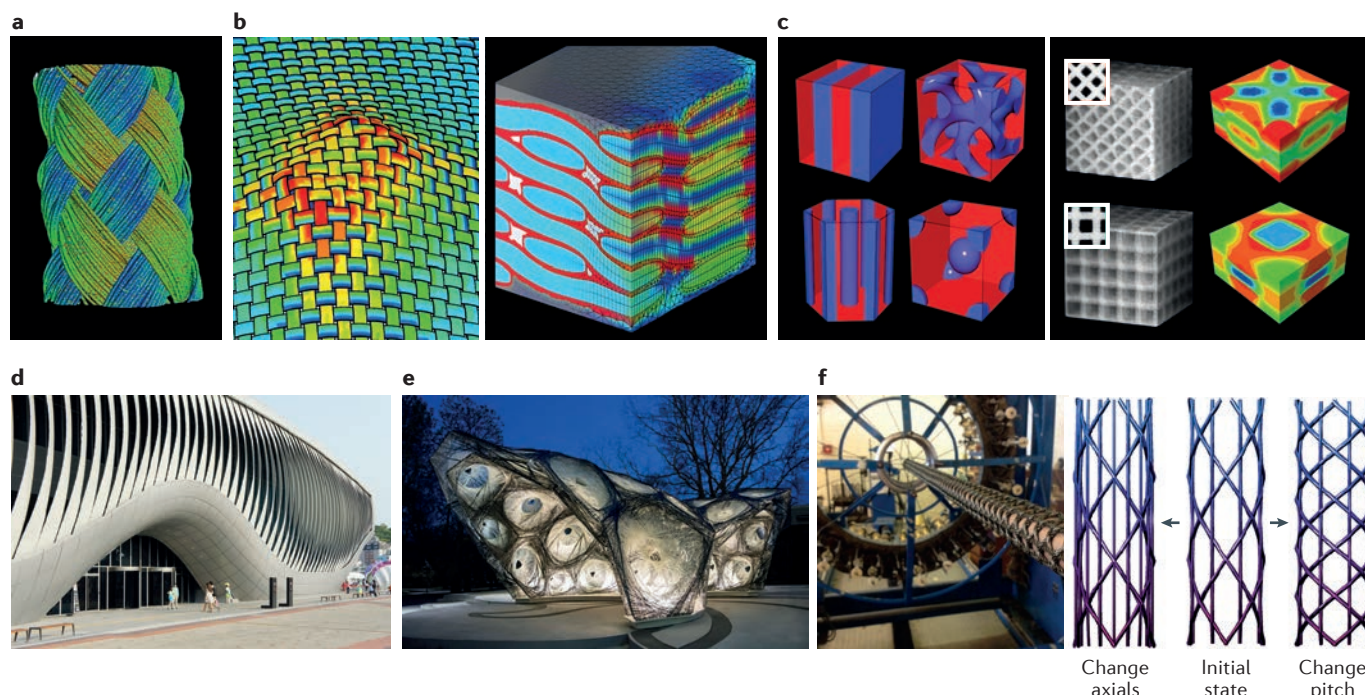


Figure 7 | Scales of analysis and design in composites science. a–c | Modern advances in composite materials characterization include tomography-based 3D reconstructions, finite element simulations of woven and fibre-reinforced geometries and additive manufacturing approaches for investigating the mechanical consequences of copolymer composites. Panel **a** shows a 3D tomographic reconstruction revealing the fibre orientation in a multiphase composite. Panel **b** shows stress contours in an impacted plain-weave Kevlar fabric (left) and in a tensile-loaded angle-interlocked C/SiC ceramic matrix composite (right; the left-hand portion of the image reveals the details of the composite architecture. Carbon-fibre tows are shown in blue; the chemical-vapour-infiltration-deposited SiC matrix is shown in red; polymer infiltration and the pyrolysed matrix are shown in grey; large pores and/or voids are shown in white. The right-hand portion of the image depicts the results from a finite element simulation). Panel **c** shows how, by combining finite element simulations (right, colour image showing the local strain contours) with direct mechanical testing performed on 3D-printed multi-material structural analogues (right, black and white image), it is possible to query the performance metrics of block copolymer nanoscale composites with complex geometries (left; the different phase-separated blocks are depicted in red and blue). **d–f** | The information gained through these characterization techniques is providing important design insight into the structural optimization of complex architectural structures, such as dynamic and morphable facades, wound carbon-fibre composite pavilions and woven 3D-network truss structures. Panel **d** shows flexible composite shading elements engineered to change shape in response to a mechanism that twists and buckles the modules. Panel **e** shows a photograph of a research pavilion constructed using a winding technique for the production of modular, double-layered fibre composite structures, which reduces the required formwork to a minimum while maintaining a large degree of geometric freedom. Panel **f** shows a braided cylindrical resin-impregnated carbon-fibre construct (left) with tunable geometries (right) for specific load-bearing applications. Panel **a** is courtesy of Jesse Garant Metrology Center, USA. Panel **b** is courtesy of G. Nilakantan, Teledyne Scientific and Imaging, USA. Panel **c** (right) is adapted with permission from REF. 123, Wiley-VCH. Panel **c** (left) is adapted from Scherer, M. R. J., *Double-Gyroid-Structured Functional Materials* (Springer, 2013) under a Creative Commons license [CC BY 3.0](#). Panel **d** is courtesy of S. Rutzinger, soma architecture, Austria. Panel **e** is courtesy of J. Knippers and A. Menges, University of Stuttgart, Germany. Panel **f** is courtesy of A. Gurley, Auburn University, USA, and adapted with permission from reference REF. 124, The American Society of Mechanical Engineers.

or other materials to protect the structural fibres and maintain a clean appearance⁸⁶. In their native form, these structural membrane systems are poor insulators, but the integration of aerogel interlayers can significantly improve their thermal performance; these aerogel blankets have a thermal conductivity of 9–16 mW mK⁻¹, which is almost half that of conventional building insulation materials^{87,88}. Despite these advantages, except for highly specialized applications in which thicker insulation layers for retrofitting are

simply not an option, the cost of aerogel production remains prohibitive for widespread use in construction: in 2012 in the United States, the cost was approximately 18 times higher compared with achieving the same insulation with conventional polymer foam insulation⁸⁷. Other efforts to broaden the performance range of these tensile membranes include the development of new thermally responsive materials with small pores that open and close in response to temperature changes in the 20–40 °C range⁸⁹.

Although tensile membranes remain a niche material in building design, other industries, such as sail production, have a more consistent demand. Inspired by recent advances in materials design for the sailing industry, traditional broad-seaming of fabric panels, still the norm for architectural membranes, could be replaced by the lamination of Mylar films over CNC-configurable moulds in conjunction with automated fibre (such as Kevlar and carbon) placement machines⁹⁰. These automated production approaches are valuable when shape variations remain within a narrow range (many sails have triangular forms with only slightly changing contours and curvature distributions). This allows the design of moulds that permit small curvature adjustments; the robotic fibre placement along the principal stresses optimizes strength-to-weight and strength-to-stiffness ratios.

Instead of focusing on how composites add value in other industries (for example, strength-to-weight ratio, stiffness, durability and dampening properties), designers have pursued solutions that turn other properties or process characteristics into a unique argument for the use of fibre-reinforced composites. For example, the ability to design composite layup systems with precisely engineered degrees of compliance was used in the design of an adaptive facade for the 2012 'One Ocean' pavilion for the Yeosu EXPO in Korea (FIG. 7d). The engineers developed glass-fibre-reinforced polymeric lamellae that could change shape through a precisely orchestrated rotation of their end constraints. In response to the rotation, the lamellae bent elastically, storing the energy initially used to create the deformation such that, upon reversing the motion, a portion of this energy could be recuperated through the servo actuation mechanism⁹¹. During the design phase of this facade, one of the main challenges was the reliability of the computational modelling, realized using nonlinear finite element analysis. Under dynamic and unpredictable loading regimes, the servo-controlled end constraints were also used to stabilize the 108 lamellae in response to dynamic wind loads, which were measured in real time. In the final product, the lamellar envelope could either configure into a completely open facade or form a smooth, closed surface.

A unique opportunity for the expanded use of synthetic composites in architectural contexts is rooted in the fully customizable processes available to designers and engineers to layer and adhere filaments, rovings or mat-based fibres into a solid form (FIG. 7e). In one such application, six-axis robotic manipulators were programmed to wind resin-coated rovings over an array of 2D ribs that described the edges of a series of doubly curved surfaces^{26,92}. By laying the fibres in multidirectional layers, a load-bearing structure could be generated. This fabrication approach has been demonstrated on site with a preformed rib structure, much like a mandrel used in filament winding, mounted on a rotating seventh axis. The equivalent off-site pre-fabrication approach relies on the synchronous movements of two six-axis robots that wind fibres over a system of 2D ribs to form tileable hexagonal modules, which are then assembled on site.

In addition to the use of carbon fibre in planar composites and free-form pavilions, braided carbon-fibre-reinforced cylindrical geometries (FIG. 7f) have gained increased attention within the architecture community. In these applications, large-scale fibre braiding machines can be used to optimize strand winding geometries for specific load-bearing applications. Recently, these approaches have also been adapted for the production of novel branched geometries⁹³ for use in lightweight structurally complex support beams and trusses.

In a 3D-printing context, the production of synthetic composites comes in the form of affordable desktop fused filament fabrication devices that use a thermoplastic composite filament of carbon-strand and nylon in conjunction with continuous fibreglass, carbon-fibre or Kevlar filaments for the production of engineering-grade components with high strength-to-weight ratios⁹⁴. However, large-scale commercial applications of this technology are still pending.

Polymers

Polymers (FIG. 8) have been integral to the production of the modern composite systems discussed above^{95,96}. PVC, despite concerns about its impact on health, is among the most widespread polymers used, with applications in window profiles, claddings, interior floor finishes and water pipes. However, recovering PVC after building renovation or demolition remains challenging. This is in part due to technical difficulties in processing recycled PVC in safe and environmentally friendly ways⁹⁷, but also attributable to a lack of economic incentives for recycling. Research in this area has not extensively involved designers, and excitement in the design community after the first emergence of polymers, or 'plastics', quickly focused on furniture design, an area in which designers were finally able to enjoy almost unlimited formal freedom.

However, apart from PVC, it is silicone rubbers that likely have had the most profound, yet largely unrecognized, impact on building construction. They have allowed for the rapid, yet permanent, adhesive bonding of large expanses of glass to their metal substructures, along with many other applications, including the watertight sealing of roofs, kitchens, and bathroom walls and floors. Contemporary city skylines of glass skyscrapers would be unthinkable without silicones. However, silicone bonds materials so effectively and durably that a separation of parts for reuse and recycling is costly and labour intensive, making landfilling the common option for demolition waste of glass curtain walls.

A new generation of designers has rediscovered the opportunities inherent in polymeric materials and the properties enabled by advances in chemistry and materials science (FIG. 8a–d). This interest was in part triggered by the development of shape-memory polymers as solids and foams. Shape-memory polymers are being explored on the furniture scale⁹⁸ (FIG. 8g), with a growing interest in collaborative endeavours between materials scientists and designers to investigate larger forms.

Polymers (including both thermoplastics and thermosets) have also had a key role in enabling 3D printing

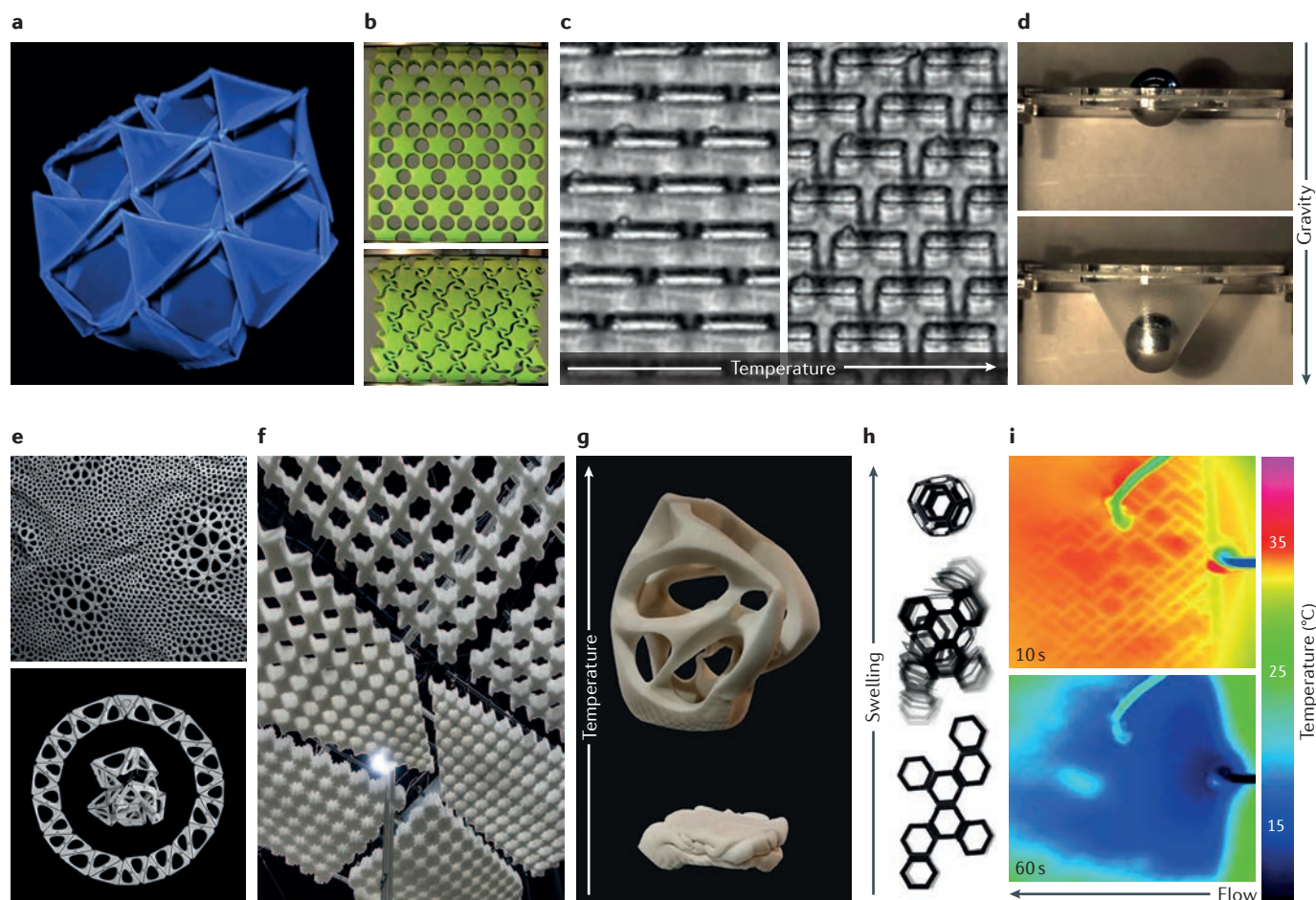


Figure 8 | Polymer research from the nanoscale to the macroscale. a–d | From self-folding millimetre-scale origami prototypes and computationally optimized auxetic metamaterials to environmentally responsive and ultra-tough composite hydrogels, recent advances in chemistry and materials science have significantly broadened the range of polymeric materials available to the design community. Panel **a** shows a confocal fluorescence micrograph of a 1 mm-wide self-folding 3D octahedron–tetrahedron polymeric truss. Panel **b** shows a photograph of a 10 cm-wide auxetic elastomeric metamaterial in the expanded (top) and buckled (bottom) configuration. Panel **c** shows an optical micrograph of an ordered array of bendable microscale plate-like structures surrounded by a thermally responsive hydrogel. Panel **d** shows photographs of a tough and highly extensible composite hydrogel, composed of an interpenetrated network of alginate and polyacrylamide chains¹²⁵, during an impact test with a steel ball with a diameter of 2 cm. **e** | The combination of computational modelling and high-resolution laser sintering of robust thermoplastics has facilitated the generation of fully collapsible and space-optimized geometries for the production of flexible-jointed 3D-printed fabrics and forms. **f–i** | Similar translational work has resulted in the production of auxetic facades with coordinated actuation, self-expanding thermally actuated shape-memory and self-folding geometries, and temperature-regulating millifluidic windows. Panel **f** shows a large-scale actuable auxetic facade consisting of water-jetted polyurethane foam panels, each with an area of $\sim 1 \text{ m}^2$. Panel **g** shows an expandable 3D structure made of a shape-memory polymer foam. Panel **h** shows a 3D-printed self-folding polyhedron; the folding is driven by differential bending within its water-swellaible hinge units. Panel **i** shows thermal images of a polydimethylsiloxane-based millifluidic vascular network veneer for the cooling of window surfaces in hot climates. The cooling effect of the water-filled channels is demonstrated over a 1 minute time frame. Panel **a** is adapted with permission from REF. 126, Wiley-VCH. Panel **b** is adapted with permission from REF. 127, Royal Society of Chemistry. Panel **c** is courtesy of J. Aizenberg, Harvard University, USA. Panel **d** is courtesy of the Wyss Institute at Harvard University, USA. Panel **e** top (title: Kinematics dress 2, detail) and bottom are courtesy of *Nervous System*, USA. Panel **g** is courtesy of *Noumenon*. Panel **h**, 4D printing, is courtesy of the Self-Assembly Lab, MIT + Stratasys Ltd + Autodesk. Panel **i** is adapted with permission from REF. 103, Elsevier.

technologies. They were among the first materials to be printed using fused filament fabrication approaches and, in recent years, more advanced 3D printers have enabled the simultaneous deposition of multiple polymeric materials. Designers with a strong interest in

computational form-finding and pattern generation methods have exploited this opportunity to create novel aesthetic expressions at the 0.5 m-size scale⁹⁹. In addition, recent 3D printing advances in the field of selective laser sintering of polymeric materials has permitted the

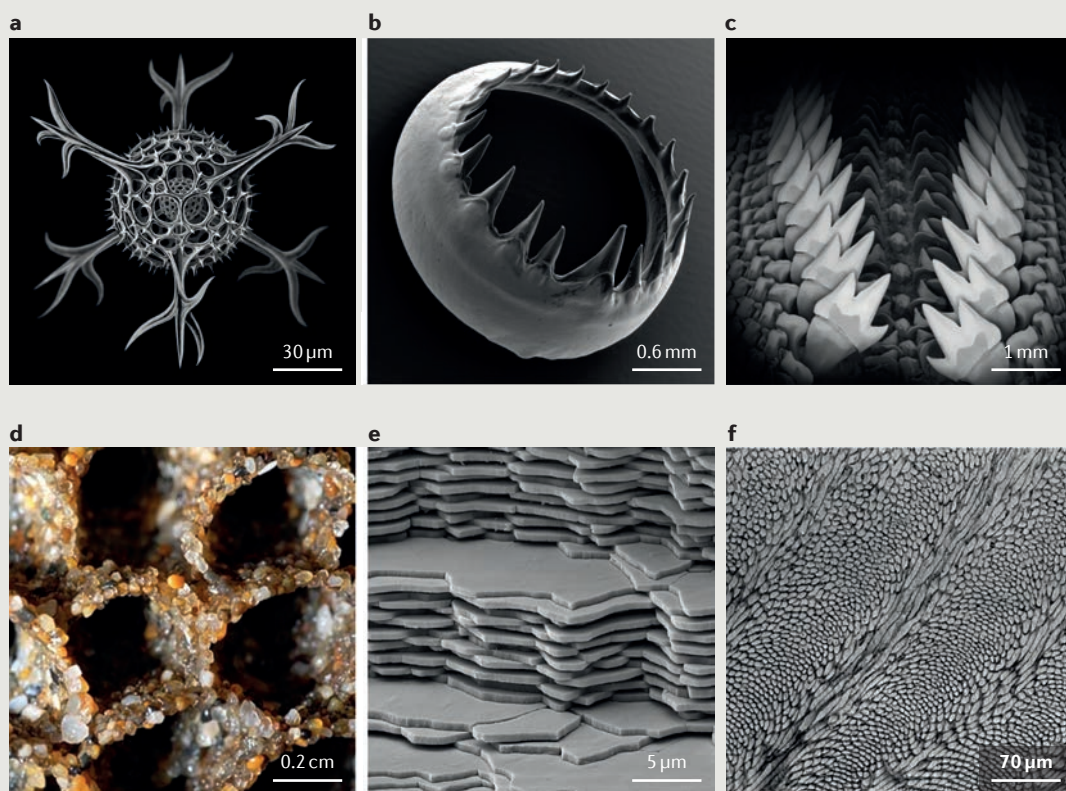
development of efficient methods for the exploration of novel design spaces. For example, the use of custom-designed packing optimization algorithms has permitted the production of parametric linkage systems for the fabrication of hinged fabric-like assemblies that move in a similar way to their fibre-based counterparts and can be printed in a pre-folded state for maximum space utilization within the 3D printing build envelope (FIG. 8e). The exploration of 3D-printed polymer designs continues with the study of swellable polymers that serve

as actuators of multimaterial 3D prints when these are submerged in water^{100,101} (FIG. 8h). If they are paired with their non-swellable counterparts, the expansion of these hydrophilic materials can be used to generate angular and other geometrical changes; the underlying principles are conceptually similar to those discussed earlier in the context of wood.

On the structural design side, low-modulus polymers, such as elastomers and foams, have been successfully used to produce auxetic metamaterials in which

Box 1 | Architectural and design inspiration from nature: the structural complexities of biological systems

Nature produces a remarkable diversity of high-performance composites, including elaborate glassy 3D constructs, high-modulus biological thermoplastics, abrasion-resistant cutting and grinding tools, underwater adhesives for granular assembly and lamellar structures, and fibrillar high-toughness organic–inorganic hybrid composites. Panel **a** of the figure shows an illustration of the spherically symmetrical glassy skeletal system of a unicellular radiolarian. Panel **b** displays a scanning electron micrograph of an individual toothed sucker ring (in this case from the Humboldt squid), which line the arms and tentacles of squid and cuttlefish, and provide additional gripping power during prey capture and handling. These materials are entirely proteinaceous and are one of the only known examples of a biological thermoplastic. The scanning electron micrograph in panel **c** shows highly mineralized and abrasion-resistant radular teeth from a chiton, a herbivorous marine mollusc that has the surprising capacity of eroding away the rocky substrates on which it grazes. The teeth are a hybrid composite of magnetite crystallites, polysaccharides and proteins, and is one of the hardest known biominerals. The photograph in panel **d** displays a honeycomb-like aggregate of tubes formed by colonial sandcastle worms, which consist of sand grains bound together by a porous, high-strength polymeric adhesive that cures underwater. The scanning electron micrograph in panel **e** illustrates the tough, laminated nanocomposite that constitutes the inner mother of pearl layer from an abalone shell. Finally, the scanning electron micrograph in panel **f** shows the complex multi-axial organization of calcium phosphate nanorods that constitute the enamel of mammalian teeth. Panel **a** is adapted from E. Haeckel, *Kunstformen der Natur*/Wikimedia Commons/Public Domain. Panel **b** is adapted with permission from REF. 111, Wiley-VCH. Panel **c** is adapted from REF. 112 under a Creative Commons license CC BY 3.0. Panel **d** is courtesy of G. McDonald, Santa Cruz, USA. Panel **e** is adapted from REF. 113, Wiley-VCH. Panel **f** is courtesy of J. C. Weaver, D. Green and T. M. Smith, Harvard University, USA.



buckling is deliberately used to produce geometrically adaptive materials. The resulting patterns (FIG. 8b) can be designed and analysed by materials scientists using non-linear finite element analysis methods¹⁰²; in collaboration with designers, this led to the fabrication of large-scale prototyping and actuation methods for the production of pavilion-scale installations based on the use of auxetic polymer foams¹²⁸ (FIG. 8f). The adaptive elements feature the blending of multiple patterns and the adjustment of pattern distributions to irregular element shape.

Polymers have also served as interlayers in glazing systems, and silicones, such as polydimethylsiloxane (PDMS), are of particular interest because they can be easily bonded to glass. Research on PDMS-based vascular networks, for example, has shown that glazing systems enhanced with a millimetre-thin PDMS layer containing liquid channels can be used to effectively cool glass exposed to solar radiation (FIG. 8i). This system can enhance thermal comfort by reducing radiant heat transfer close to the glass element, as well as potentially reducing cooling loads for secondary building-level cooling systems by transferring a portion of the incoming solar energy to the water-based vascular network¹⁰³. An extension of this approach is to increase the depth of the vascular system and form light-modulating lamellae that are functionally similar to window blinds or louvers¹⁰⁴. Shearing of the opposing panes of glass deforms the PDMS lamellae such that light can be reflected and refracted to a desired area in a controlled manner. The capability of the system to redirect light to deeper areas of a space has been experimentally demonstrated — a potential advantage in the traditionally deep US office space where electrical lighting is needed for most of the floor surface owing to a lack of available daylight.

Summary and outlook

Materials and architecture have a reciprocal relationship. New materials developments have been the enabling factor in a range of historic advancements in the construction of the built environment. These developments have made possible new structural forms, such as long-spanning glued laminated timber systems, high-rise buildings made of high-strength steel, and reinforced-concrete shell structures. Materials innovation has also given us new environmental capacities, including the ability to construct glazing systems for efficient daylighting illumination of interiors, which improve working and living conditions. Other materials developments have extended the range of design expressions in the quest for more aesthetically compelling spaces. Often, materials science responds to the needs formulated by architects, engineers and builders, but in other cases, materials innovation first takes place outside the building industry and, once adopted, transforms design and construction practices.

Recently, the relationship between the design profession and materials science has changed, and designers are more actively engaged in the exploration of the opportunities inherent in both materials properties and materials processes. Harvard University's Adaptive Living Environments (ALivE) group has developed

a successful approach that does not necessarily start with the intention of solving a problem, but instead frequently takes the opposite approach, whereby designers and scientists collaborate to unravel the design and performance opportunities afforded by materials systems. This approach, also described as 'hacking science' (REF. 105), develops application areas for novel materials systems through a range of design experimentations. Prototypical installations and research pavilions have become the primary output mode of this type of work, which involves materials scientists, chemists and biologists as core members of the design teams. Materials exploration today is also deeply affected and enhanced by advanced computational techniques and digitally controlled prototyping and fabrication processes. These 'digital materials' hold much promise for smarter and more deliberate use of precious resources¹⁰⁶, and may also lead to a shift in materials consumption towards materials types with reduced environmental impact and lower carbon emissions.

Efforts to develop natural materials systems to substitute existing materials for structural and non-structural applications are spreading¹⁰⁷. A related young but growing area is focused on the development of reliable approaches to use biological systems for the direct production of engineered forms as a replacement or supplement for conventional building materials. Examples include the directed growth of fungal mycelium in confined spaces for the production of lightweight structural components¹⁰⁸ and the guided growth of trees for the generation of custom furniture¹⁰⁹. At the more established end of this biological production continuum, bacteria have long contributed to producing viscosifiers for concrete and grout; however, the quest to replace in more substantial quantities construction materials with high carbon footprints is still in the early stages⁴⁹. The use of enzymes such as urease to catalyse the formation of brick-like constructs from simple precursor materials shows some promise¹¹⁰, but as of yet, very few of these approaches have advanced to a stage at which commercial applications, such as structural bricks, are feasible. Many of these explorations are still in their infancy, but they point to a possible future in which biological production from the microscale to the macroscale will be an indispensable part of a broadened set of construction activities.

Other recent research efforts are driven by a strong interest in the study of natural precedents as aesthetic or performative inspirations, an approach often referred to as 'biomimicry' by the design community. As a result, both designers and research scientists are taking a renewed interest in the way natural systems grow and function, and over the past 20 years, there have been many remarkable discoveries and architectural insights that have resulted from the direct investigation of structure–function relationships in biological systems (BOX 1). Nature has had billions of years to evolve elegant solutions that are well adapted to specific environmental constraints, and the analysis of these structures and processes can serve as a powerful source to guide the work of materials scientists and designers alike.

1. Addington, M. & Schodek, D. *Smart Materials and Technologies: For the Architecture and Design Professions* (Routledge, 2005).
2. Knippers, J., Nickel, K. & Speck, T. *Biomimetic Research for Architecture and Building Construction* (Springer, 2016).
3. Picon, A. & Thom, M. *French Architects and Engineers in the Age of Enlightenment* (Cambridge Univ. Press, 1992).
4. Elliott, C. D. *Technics and Architecture: the Development of Materials and Systems for Buildings* (MIT Press, 1992).
5. Schodek, D. L., Bechthold, M., Kao, K., Griggs, K. & Steinberg, M. *Digital Design and Manufacturing* (Wiley, 2005).
6. Ashby, M. F., Ferreira, P. J. & Schodek, D. L. *Nanomaterials, Nanotechnologies and Design* (Elsevier, 2009).
7. Sabin, J. & Santangelo, C. in *MRS Symposium Proceedings Vol. 1800* (Cambridge Univ. Press, 2015).
8. Gutierrez, M. P. & Lee, L. P. Multiscale design and integration of sustainable building functions. *Science* **341**, 247–248 (2013).
9. Sellers, T. *Plywood and Adhesive Technology* (CRC Press, 1985).
10. Marra, A. A. *Technology of Wood Bonding* (Springer, 1992).
11. van den Kuilen, J. G., Zhouyan, A. C. & Minjuan, H. Very tall wooden buildings with cross laminated timber. *Procedia Eng.* **14**, 1621–1628 (2011).
12. Harries, K. S. & Sharma, B. *Nonconventional and Vernacular Construction Materials: Characterisation, Properties and Applications* (Woodhead Publishing, 2016).
13. Wang, Z., Li, Z., Gu, Z., Hong, Y. & Cheng, L. Preparation, characterization and properties of starch-based wood adhesive. *Carbohydr. Polym.* **88**, 699–706 (2012).
14. Dorr, D. N., Frazier, S. D., Hess, K. M., Traeger, L. S. & Sruhar, W. V. Bond strength of biodegradable gelatin-based wood adhesives. *J. Renewable Mater.* **3**, 195–204 (2015).
15. Haag, A. P., Geesey, G. G. & Mittleman, M. W. Bacterially derived wood adhesive. *Int. J. Adhes. Adhes.* **26**, 177–183 (2006).
16. Hahn, B., Vallée, T., Stamm, B. & Weinand, Y. Moment resisting connections composed of friction-welded spruce boards: experimental investigations and numerical strength prediction. *Eur. J. Wood Prod.* **72**, 229–241 (2014).
17. Stamm, B., Natterer, J. & Navi, P. Joining wood by friction welding. *Holz Roh-Werkst.* **63**, 313–320 (2005).
18. Lee, S.-H. & Wang, S. Biodegradable polymers/bamboo fiber biocomposite with bio-based coupling agent. *Composites Part A* **37**, 80–91 (2006).
19. Bao, L., Chen, Y., Zhou, W., Wu, Y. & Huang, Y. Bamboo fibers poly(ethylene glycol)-reinforced poly(butylene succinate) biocomposites. *J. Appl. Polym. Sci.* **122**, 2456–2466 (2011).
20. Strode, W. & Dean, D. L. *Experiments With a Single Layer Plywood Monkey Saddle Shell* (Univ. Kansas Publications, 1961).
21. Krauss, F. *Hyerbolische paraboloide Schalen aus Holz [German]* (Krämer, 1969).
22. Bechthold, M. Wood-foam sandwich shells: computer-aided manufacturing of complex shapes. *J. Int. Assoc. Shell Spatial Struct.* **44**, 679–690 (2002).
23. Dawson, C., Vincent, J. F. V. & Rocca, A.-M. How pine cones open. *Nature* **390**, 668 (1997).
24. Elbaum, R., Zaltzman, L., Burgert, I. & Fratzl, P. The role of wheat awns in the seed dispersal unit. *Science* **316**, 884–886 (2007).
25. Harrington, M. J. *et al.* Origami-like unfolding of hydro-actuated ice plant seed capsules. *Nat. Commun.* **2**, 537 (2011).
26. Menges, A. & Reichert, S. Performative wood: physically programming the responsive architecture of the HygroScope and HygroSkin projects. *Architectural Design* **85**, 66–73 (2015).
27. Wood, D. M., Correa, D., Krieg, O. D. & Menges, A. Material computation — 4D timber construction: towards building-scale hygroscopic actuated self-constructing timber surfaces. *Int. J. Arch. Comput.* **14**, 49–62 (2016).
28. Tarkow, H. & Turner, H. The swelling pressure of wood. *For. Prod. J.* **8**, 193–197 (1958).
29. Reichert, S., Menges, A. & Correa, D. Meteorosensitive architecture: biomimetic building skins based on materially embedded and hygroscopically enabled responsiveness. *Comput. Aided Design* **60**, 50–69 (2015).
30. Correa, D. *et al.* 3D-printed wood: programming hygroscopic material transformations. *3D Print. Add. Manufact.* **2**, 106–116 (2015).
31. Bechthold, M., Kane, A. & King, N. *Ceramic Material Systems* (Birkhäuser, 2015).
32. King, N., Bechthold, M., Kane, A. & Michalatos, P. Robotic tile placement: tools, techniques and feasibility. *Auto. Constr.* **39**, 161–166 (2013).
33. Van Aubel, M. Ceramic foam. US Patent 20150018195 (2015).
34. Bernardo, E., De Lazzari, M., Colombo, P., Llaudis, A. S. & Garcia-Ten, F. J. Lightweight porcelain stoneware by engineered CeO₂ addition. *Adv. Eng. Mater.* **12**, 65–70 (2010).
35. Diegel, O., Withell, A., de Beer, D., Potgier, J. & Noble, F. Low-cost 3D printing of controlled porosity ceramic parts. *Int. J. Auto. Technol.* **6**, 618–626 (2012).
36. Bechthold, M., King, N., Kane, A. O., Niemasz, J. & Reinhart, C. in *Proc. 28th ISARC, Seoul, Korea 70–75* (2011).
37. Bechthold, M. Prototipos cerámicos — diseño, computación y fabricación digital [Spanish]. *Inf. Constr.* **68**, 91–102 (2016).
38. Moon, J., Grau, J. E., Knezevic, V., Cima, M. J. & Sachs, E. M. Ink-jet printing of binders for ceramic components. *J. Am. Ceram. Soc.* **85**, 755–762 (2002).
39. Grinham, J., Blabolil, R. & Haak, J. Harvest shade screens: programming material for optimal energy building skins. *ACADIA* http://papers.cumincad.org/data/works/att/acadia14_281_content.pdf (2014).
40. Castellano, M. G., Indirli, M. & Martelli, A. Progress of application, research and development, and design guidelines for shape memory alloy devices for cultural heritage structures in Italy. *Proc. SPIE* <https://dx.doi.org/10.1117/12.434124> (2001).
41. Nieve, P. Construction steelwork makes its 3D printing premiere. *Arup* <https://www.arup.com/news-and-events/news/construction-steelwork-makes-its-3d-printing-premiere> (2014).
42. Baker, R. Method of making decorative articles. US Patent 1533300A (1925).
43. Warton, J., Dwivedi, R. & Kovacevic, R. in *Robotic Fabrication in Architecture, Art and Design 2014* (eds McGee, W. & de Leon, M. P.) 147–161 (Springer, 2014).
44. Skylar-Scott, M. A., Gunaesekaran, S. & Lewis, J. A. Laser-assisted direct ink writing of planar and 3D metal architectures. *Proc. Natl Acad. Sci. USA* **113**, 6137–6142 (2016).
45. Ribeiro, F., Norrish, J. & McMaster, R. S. Practical case of rapid prototyping using gas metal arc welding. *Repositorium* <http://repositorium.sdum.uminho.pt/bitstream/1822/31411/1/04%20PARIS.pdf> (1994).
46. Ribero, F. & Norrish, J. Making components with controlled metal deposition. *Proc. IEEE Int. Symp. Ind. Electron.* <https://dx.doi.org/10.1109/ISIE.1997.648647> (1997).
47. Kind-Barkauskas, F., Kauhens, B., Polónyi, S. & Brandt, J. *Beton Atlas [German]* 2nd edn (Walter de Gruyter, 2002).
48. Jones, B. E. *Cassell's Reinforced Concrete* (Cassell and Co., 1913).
49. Plank, J. Applications of biopolymers and other biotechnological products in building materials. *Appl. Microbiol. Biotechnol.* **66**, 1–9 (2004).
50. Raki, L., Beaudoin, J., Alizadeh, R., Makar, J. & Taijiro, S. Cement and concrete nanoscience and nanotechnology. *Materials* **3**, 918–942 (2010).
51. Richard, P. in *Proc. 4th Int. Symp. Utilization High-Strength/High-Performance Concrete* (eds de Larrard, F. & Lacroix, R.) 1343–1357 (1996).
52. Russel, H. G. & Graybeal, B. A. Ultra-high performance concrete: a state-of-the-art report for the bridge community U.S. Department of Transportation, Federal Highway Administration <https://www.fhwa.dot.gov/publications/research/infrastructure/structures/hpc/13060/13060.pdf> (2013).
53. Forstlechner, F. X., Freytag, B. & Peters, S. Spannbettvorspannung dünner Carbonbeton-Platten [German]. *Beton- Stahlbetonbau* **110**, 419–428 (2015).
54. Means, R. *2016 Building Construction Cost Data Book 74th edn* (ed. Plotner, S. C.) (RS Means, 2016).
55. Amtsberg, F., Parmann, G., Trummer, A. & Peters, S. in *Robotic Fabrication in Architecture, Art and Design 2016* (eds Reinhardt, D., Saunders, R. & Burry, J.) 304–315 (Springer, 2016).
56. Bock, T. Construction robotics. *Auto. Robots* **22**, 201–209 (2007).
57. Wheen, R. J. & Bridge, R. Q. ORIHUNE-the World's first folded concrete canoe. *J. Ferrocement* **11**, 311–318 (1981).
58. Bechthold, M. in *Proc. IASS Symp. Shell and Spatial Structures: Structural Architecture 53–56* (IASS, 2007).
59. Redjivani, A. *WO/1993/020990A1* (1993).
60. Guerrini, G. L. & Roberta, A. *EP1957245* (2014).
61. Lloret, E. *et al.* Complex concrete structures: merging existing casting techniques with digital fabrication. *Comput. Aided Design* **60**, 40–49 (2015).
62. Penja, J. Exploratory investigation of solid freeform construction. *Auto. Constr.* **5**, 427–437 (1997).
63. Dini, E., Chiarugi, M. & Nannini, R. Method and device for building automatically conglomerate structures. US Patent 20080148683 A1 (2008).
64. Cesaretti, G., Dini, E., De Kestelier, X., Colla, V. & Pambaguian, L. Building components for an outpost on the Lunar soil by means of a novel 3D printing technology. *Acta Astronaut.* **93**, 430–450 (2014).
65. Koshnevis, B. & Dutton, R. Innovative rapid prototyping process makes large sized, smooth surfaced complex shapes in a wide variety of materials. *Mater. Technol.* **13**, 52–56 (1998).
66. Koshnevis, B. *et al.* Lunar habitat construction — a novel technique for ISRU-based habitat development. *Aero. Sci. Meetings* <https://dx.doi.org/10.2514/6.2005-538> (2005).
67. Koshnevis, B. Automated construction by contour crafting — related robotics and information technologies. *Auto. Constr.* **13**, 5–19 (2004).
68. Le, T. T. *et al.* Mix design and fresh properties for high-performance printing concrete. *Mater. Struct.* **45**, 1221–1232 (2012).
69. Lim, S. *et al.* Developments in construction-scale additive manufacturing processes. *Auto. Constr.* **21**, 262–268 (2012).
70. Buswell, R. A., Thorpe, A., Soar, R. C. & Gibb, A. F. Design, data and process issues for mega-scale rapid manufacturing machines used for construction. *Auto. Constr.* **17**, 923–929 (2008).
71. Le, T. T. *et al.* Hardened properties of high-performance printing concrete. *Cem. Concr. Res.* **42**, 558–566 (2012).
72. Feng, P., Meng, X., Chen, J.-F. & Ye, L. Mechanical properties of structures 3D printed with cementitious powders. *Constr. Build. Mater.* **93**, 486–497 (2015).
73. Kim, T., Tae, S. & Roh, S. Assessment of the CO₂ emission and cost reduction performance of low-carbon-emission concrete mix design using an optimal mix design system. *Renewable Sustainable Energy Rev.* **25**, 729–741 (2013).
74. Hub, A., Zimmermann, G. & Knippers, J. Leichtbeton mit Aerogelen als Konstruktionswerkstoff [German]. *Beton Stahlbetonbau* **108**, 654–661 (2013).
75. Schlaich, M. & Hückler, A. Infralichtbeton 2.0 [German]. *Beton Stahlbetonbau* **107**, 757–766 (2012).
76. Herrman, M. & Sobek, W. Gradientenbeton — Numerische Entwurfsmethoden und experimentelle Untersuchung gewichtsoptimierter Bauteile [German]. *Beton Stahlbetonbau* **110**, 673–686 (2015).
77. Ge, D. *et al.* Robust smart window: reversible switching from high transparency to angle-independent structural color display. *Adv. Mater.* **27**, 2489–2495 (2015).
78. Kim, P. *et al.* Rational design of mechano-responsive optical materials by fine tuning the evolution of strain-dependent wrinkling patterns. *Adv. Opt. Mater.* **1**, 381–388 (2013).
79. Marchelli, G., Prabhakar, R., Storti, D. & Ganter, M. The guide to glass 3D printing: developments, methods, diagnostics and results. *Rapid Prototyp. J.* **17**, 187–194 (2011).
80. Klein, J. *et al.* Additive manufacturing of optically transparent glass. *3D Print. Addit. Manufact.* **2**, 92–105 (2015).
81. Sheil, B., Menges, A., Glynn, R. & Skavara, M. Fabricate: rethinking design and construction. University College London <https://www.ucl.ac.uk/bartlett/architecture/case-studies/2017/apr/fabricate-2017-rethinking-design-and-construction> (2017).
82. Bakis, C. E. *et al.* Fiber-reinforced polymer composites for construction — state-of-the-art review. *J. Compos. Constr.* **6**, 73–87 (2002).
83. John, M. J. & Thomas, S. Biofibers and biocomposites. *Carbohydr. Polym.* **71**, 343–364 (2008).
84. Faruk, O., Bledzki, A. K., Fink, H.-P. & Sain, M. Biocomposites reinforced with natural fibers: 2000–2010. *Prog. Polym. Sci.* **37**, 1552–1596 (2012).
85. Lee, S.-H. & Wang, S. Biodegradable polymers/bamboo fiber biocomposite with bio-based coupling agent. *Composites* **37**, 80–91, (2006).

86. Koch, K.-M. *Membrane Structures: the Fifth Building Material* (Prestel, 2004).
87. Koebel, M., Rigacci, A. & Achard, P. Aerogel-based thermal superinsulation: an overview. *J. Sol-Gel Sci. Technol.* **63**, 315–339 (2012).
88. Augustyniak, M. J. & McCoy, T. D. Architectural membrane and method of making same. USA Patent 8899000 B2 (2014).
89. Park, Y., Gurierrez, M. P. & Lee, L. P. Reversible self-actuated thermo-responsive pore membrane. *Sci. Rep.* **6**, 39402 (2016).
90. Keire, F. A. Sail of woven material and method of manufacture. USA Patent 6257160 B1 (2001).
91. Knippers, J., Jungjohann, H., Scheible, F. & Oppe, M. Bio-inspirierte kinetische Fassade fuer den Themenpavillon "one ocean" EXPO 2012 in Yeosu. Korea [German]. *Bautechnik* **90**, 341–347 (2013).
92. Waimer, F. *et al.* Bionisch-inspirierte Faserverbundstrukturen [German]. *Bautechnik* **90**, 766–771 (2013).
93. Masselter, T. *et al.* Biomimetic optimisation of branched fibre-reinforced composites in engineering by detailed analyses of biological concept generators. *Bioinspir. Biomim.* **11**, 055005 (2016).
94. Mark, G. T. Methods for fiber reinforced additive manufacturing. US Patent 20140361460 A1 (2014).
95. Engelsmann, S., Spalding, V. & Peters, S. *Kunststoffe in Architektur und Konstruktion* [German] (Birkhäuser, 2010).
96. Bell, M. & Buckley, C. *Permanent Change: Plastics in Architecture and Engineering* (Princeton Arch. Press, 2014).
97. Pacheco-Torgal, F., Jalali, S. & Fucic, A. *Toxicity of Building Materials* (Woodhead, 2012).
98. Fan, J.-N. & Schodek, D. Personalized furniture within the conditions of mass production. *Academia* http://www.academia.edu/1576646/Personalized_furniture_within_the_condition_of_mass_production (2007).
99. Oxman, N., Keating, S. & Tsai, E. in *Innovative Developments in Virtual and Physical Prototyping* (ed. da Silva Bartolo, P. J.) 483–489 (2011).
100. Tibbitts, S. & Cheung, K. Programmable materials for architectural assembly and automation. *Assembly Auto.* **32**, 216–225 (2012).
101. Tibbitts, S. 4D printing: multi-material shape change. *Arch. Design* **84**, 116–121 (2014).
102. Babae, S. *et al.* 3D soft metamaterials with negative Poisson's ratio. *Adv. Mater.* **25**, 5044–5049 (2013).
103. Hatton, B. D. *et al.* An artificial vasculature for adaptive thermal control of windows. *Sol. Energy Mater. Sol. Cells* **117**, 429–436 (2013).
104. Park, D. *et al.* Dynamic daylight control system implementing thin cast arrays of polydimethylsiloxane-based millimeter-scale transparent louvers. *Build. Environ.* **82**, 87–96 (2014).
105. Bechthold, M. & Sayegh, A. Hacking science: the ALiVE group's material design methods for interdisciplinary environments. *Arch. Design* **85**, 108–113 (2015).
106. Gramazio, F. & Kohler, M. *Digital Materiality in Architecture* (Lars-Müller, 2008).
107. Ivanov, V. & Stabnikov, V. *Construction Biotechnology* (Springer, 2017).
108. Bayer, E. & McIntyre, G. Method for making dehydrated mycelium elements and product made thereby. US Patent US20120270302A1 (2012).
109. Dawood, S. Designer grows furniture from the ground. *Design Week* <https://www.designweek.co.uk/issues/30-march-5-april-2015/designer-grows-furniture-from-the-ground/> (2015).
110. Dosier, G. K. Methods for making construction materials using enzyme producing bacteria. US Patent US9199880B2 (2014).
111. Miserez, A. *et al.* Microstructural and biochemical characterization of the nanoporous sucker rings from *Dosidicus gigas*. *Adv. Mater.* **21**, 401–406 (2009).
112. Weaver, J. C. *et al.* Analysis of an ultra hard magnetic biomimetic in chiton radular teeth. *Mater. Today* **13**, 42–52 (2010).
113. Frolich, S., Weaver, J. C., Dean, M. N. & Birkedal, H. Uncovering nature's design strategies through parametric modeling, multi-material 3D printing, and mechanical testing. *Adv. Eng. Mater.* **19**, e201600848 (2017).
114. Ashby, M. *Materials and the Environment* (Butterworth-Heinemann, 2009).
115. Gibson, L. J., Ashby, M. F. & Harley, B. A. *Cellular Materials in Nature and Medicine* (Cambridge Univ. Press, 2010).
116. Leban, J. M. *et al.* Wood welding: a challenging alternative to conventional wood gluing. *Scand. J. For. Res.* **20**, 534–538 (2005).
117. Sang, X. & LeBeau, J. M. Revolving scanning transmission electron microscopy: correcting sample drift distortion without prior knowledge. *Ultramicroscopy* **138**, 28–35 (2014).
118. Brom, J. E. *Growth and Characterization of Bismuth Selenide Thin Films by Chemical Vapour Deposition*. Thesis, Penn. State Univ. (2014).
119. Saleh, A. A., Gazder, A. A. & Pereloma, E. V. EBSD observations of recrystallisation and tensile deformation in twinning induced plasticity steel. *Trans. Indian Inst. Met.* **66**, 621–629 (2013).
120. Dmitrieva, O. *et al.* Chemical gradients across phase boundaries between martensite and austenite in steel studied by atom probe tomography and simulation. *Acta Mater.* **59**, 364–374 (2011).
121. Ramazani, A., Mukherjee, K., Quade, H., Prahl, U. & Bleck, W. Correlation between 2D and 3D flow curve modelling of DP steels using a microstructure-based RVE approach. *Mater. Sci. Eng. A* **560**, 129–139 (2013).
122. Lanzón, M., Cnudde, V., de Kock, T. & Dewanckele, J. X-Ray microtomography (μ -CT) to evaluate microstructure of mortars containing low density additions. *Cem. Concr. Comp.* **34**, 993–1000 (2012).
123. Cho, H. *et al.* Engineering the mechanics of heterogeneous soft crystals. *Adv. Funct. Mater.* **26**, 6938–6949 (2016).
124. Gurley, A., Beale, D., Broughton, R. & Branscomb, D. The design of optimal lattice structures manufactured by maypole braiding. *J. Mech. Eng.* **137**, 101401 (2015).
125. Sun, J.-Y. *et al.* Highly stretchable and tough hydrogels. *Nature* **489**, 133–136 (2012).
126. Na, J.-H. *et al.* Programming reversibly self-folding origami with micropatterned photo-crosslinkable polymer trilayers. *Adv. Mater.* **27**, 79–85 (2015).
127. Shim, J. *et al.* Harnessing instabilities for design of soft reconfigurable auxetic/chiral materials. *Soft Matter* **9**, 8198–8202 (2013).
128. Mesa, O. *et al.* Non-linear matters: auxetic surfaces. *ACADIA* http://papers.cumincad.org/data/works/att/acadia17_392.pdf (2017).
129. Tucker, S. N. & Ambrose, M. D. Embodied energy of dwellings. *CSIRO* <https://publications.csiro.au/rpr/download?pid=procite:54757bf5-6619-4ba8-8415-4012ca2a477e&dsid=DS1> (2017).

Acknowledgements

The research presented here draws on collaborations between the Harvard Graduate School of Design, the Wyss Institute for Biologically Inspired Engineering, the Harvard Paulson School of Engineering and Applied Sciences, the Massachusetts Institute of Technology (MIT) Media Lab, the MIT Department of Civil and Environmental Engineering, the Max Planck Institute of Colloids and Interfaces, and the Nanyang Technological University School of Materials Science & Engineering. In particular, the authors thank Joanna Aizenberg, Katia Bertoldi, David Mooney, Allen Sayegh, Chuck Hoberman, Neri Oxman, Admir Masic, Peter Fratzl, Mason Dean, John Dunlop, Matt Harrington, Lorenzo Guiducci, Ali Miserez, Jack Mershon, Jonathan Grinham, Tiffany Cheng, Kelley Hess, Sarah Norman, Saurabh Mhatre, Malika Singh, Kevin Hinz, Daekwon Park, Olga Mesa, Philseok Kim, Johannes Overvelde, Jack Alvarenga, Onye Ahanotu, Kenneth Park, Benjamin Hatton and Luo Gu for their contributions to this work.

Author contributions

Both authors contributed equally to the preparation of this manuscript.

Competing interests statement

The authors declare no competing interests.

Publisher's note

Springer Nature remains neutral with regard to jurisdictional claims in published maps and institutional affiliations.

How to cite this article

Bechthold, M. & Weaver, J. C. Materials science and architecture. *Nat. Rev. Mater.* **2**, 17082 (2017).

FURTHER INFORMATION

Guided growth of trees: <http://fullgrown.co.uk/>
Nervous System: <http://nervo.us>
Noumenon: <http://www.noumenon.eu/#6panel1-1>

Figure permissions

Box 1

Panel **a** is adapted from E. Haeckel, *Kunstformen der Natur*/Wikimedia Commons/Public Domain. Panel **b** is adapted with permission from REF. 111, Wiley-VCH. Panel **c** is adapted from REF. 112 under a Creative Commons license [CC BY 3.0](#). Panel **d** is courtesy of G. McDonald, Santa Cruz, USA. Panel **e** is adapted from REF. 113, Wiley-VCH. Panel **f** is courtesy of J. C. Weaver, D. Green and T. M. Smith, Harvard University, USA.

Fig.1

The Ashby plots were generated using **Granta CES Selector** software. The pie chart is adapted with permission from REF. 114, Elsevier.

Fig.2

Panel **a** (top) is from **Albrecht Wei  er/Getty Stock Image**. Panel **a** (bottom) is courtesy of M. Eder and M. Harrington, Max Planck Institute of Colloids and Interfaces, Germany. Panels **b** and **c** are adapted with permission from REF. 24, AAAS. The scanning electron micrograph in panel **d** is courtesy of the N.C. Brown Center for Ultrastructure Studies at SUNY-ESF, Syracuse, NY; the plot is adapted from REF. 115, Cambridge University Press. Panel **e**, HygroSkin — Meterosensitive Pavilion, FRAC Centre Orleans, 2013, is courtesy of Achim Menges in collaboration with Oliver David Krieg and Steffen Reichert, Achim Menges Architect BDA, Institute for Computational Design, University of Stuttgart, Germany. Panel **f**, HygroScope — Meterosensitive Morphology, Permanent Collection of the Centre Pompidou Paris, 2012, is courtesy of Achim Menges in collaboration with Steffen Reichert, Achim Menges Architect BDA, Institute for Computational Design, Transsolar Climate Engineering. Panel **g** is adapted with permission from REF. 27, SAGE. Panel **h** (top) is courtesy of J.M. Leban, INRA, Paris, France. Panel **h** (bottom) is adapted from REF. 116, Taylor & Francis.

Fig.3

Panel **a** is courtesy of J. M. LeBeau, North Carolina State University, USA. Panel **b** is adapted with permission from REF. 118, Penn State University. Panel **c** is courtesy of J. C. Weaver and D. R. Clarke, Harvard University, USA. Panel **d** is courtesy of K. O'Kelly, Trinity College Dublin, Ireland. Panel **e** is courtesy of S. Mhatre, Harvard University, USA. Panel **f** is courtesy of T. Yamanashi, Nikken Sekkei Ltd., Japan. Panel **g** is courtesy of R. Rael, Rael San Fratello, USA. Panel **h** is courtesy of P. G  mez-Tena, Instituto de Tecnolog  a Cer  mica, Spain.

Fig.4

Panel **a** is adapted with permission from REF. 119, Springer. Panel **b** is adapted with permission from REF. 120, Elsevier. Panel **c** is adapted with permission from REF. 121, Elsevier. Panel **d** is courtesy of J. Grinham, Harvard University, USA. Panel **e** is courtesy of Arup and D. De Jong, David fotografie, Amsterdam, the Netherlands. Panel **f** is courtesy of MX3D, Amsterdam, the Netherlands.

Fig.5

Panel **a** is adapted from REF. 50 under a Creative Commons license [CC BY 3.0](#). Panels **b** and **c** are courtesy of J. C. Weaver, Harvard University, and A. Masic, Massachusetts Institute of Technology (MIT), USA. Panel **d** is adapted with permission from REF. 122, Elsevier. Panel **e** is courtesy of B. Khoshnevis, Contour Crafting Corporation, USA. Panel **f** is courtesy of S. Keating, MIT, USA; the samples were created by Steven Keating and Prof. Neri Oxman (Mediated Matter, MIT Media Lab) in collaboration with Timothy Cooke and Dr John Fern  ndez (MIT Building Technology Department). Panel **g** is courtesy of Z. Liao, Hong Kong, China.

Fig.6

Panel **c** is courtesy of **Corning Inc.**, USA. Panel **d** is from Google Street View,    2017 Google. Panel **e** is courtesy of B. Gulick and James Carpenter Design Associates Inc., USA. Panel **f** is courtesy of S. Keating, Massachusetts Institute of Technology, USA. Panel **g** is courtesy of A. Ryan, Lexington, Massachusetts, USA.

Fig.7

Panel **a** is courtesy of **Jesse Garant Metrology Center, USA**. Panel **b** is courtesy of G. Nilakantan, Teledyne Scientific and Imaging, USA. Panel **c** (right) is adapted with permission from REF. 123, Wiley-VCH. Panel **c** (left) is adapted from Scherer, M. R. J., *Double-Gyroid-Structured Functional Materials* (Springer, 2013) under a Creative Commons license [CC BY 3.0](#). Panel **d** is courtesy of S. Rutzinger, soma architecture, Austria. Panel **e** is courtesy of J. Knippers and A. Menges, University of Stuttgart, Germany. Panel **f** is courtesy of A. Gurley, Auburn University, USA, and adapted with permission from reference REF. 124, The American Society of Mechanical Engineers.

Fig.8

Panel **a** is adapted with permission from REF. 126, Wiley-VCH. Panel **b** is adapted with permission from REF. 127, Royal Society of Chemistry. Panel **c** is courtesy of J. Aizenberg, Harvard University, USA. Panel **d** is courtesy of the Wyss Institute at Harvard University, USA. Panel **e** top (title: Kinematics dress 2, detail) and bottom are courtesy of **Nervous System**, USA. Panel **g** is courtesy of **Noumenon**. Panel **h**, 4D printing, is courtesy of the Self-Assembly Lab, MIT + Stratasys Ltd + Autodesk. Panel **i** is adapted with permission from REF. 103, Elsevier.

Subject categories

Physical sciences / Materials science / Structural materials [URI /639/301/1023]

Physical sciences / Materials science / Structural materials / Metals and alloys [URI /639/301/1023/1026]

Physical sciences / Materials science / Structural materials / Ceramics [URI /639/301/1023/1024]

Physical sciences / Materials science / Structural materials / Composites [URI /639/301/1023/1025]

Physical sciences / Materials science / Structural materials / Glasses [URI /639/301/1023/218]

ToC blurb

000 Materials science and architecture

Martin Bechthold and James C. Weaver

Designer materials and advanced fabrication technologies are transforming architecture, so that architects, engineers and materials scientists now work side by side to develop innovative architectural solutions. This Review follows these developments for different materials, in particular wood, ceramics, metals, concrete, glass, synthetic composites and polymers.